

Donor–Acceptor Systems

Synthesis, Structure, and Optical Studies of Donor–Acceptor-Type Near-Infrared (NIR) Aza–Boron-Dipyrrromethene (BODIPY) Dyes

Naresh Balsukuri,^[a] Mohsin Y. Lone,^[b] Prakash C. Jha,^[b] Shigeki Mori,^[c] and Iti Gupta*^[a]

Abstract: Six donor–acceptor-type near-infrared (NIR) aza–boron-dipyrrromethene (BODIPY) dyes and their corresponding aza–dipyrrins were designed and synthesized. The donor moieties at the 1,7-positions of the aza–BODIPY core were varied from naphthyl to *N*-phenylcarbazole to *N*-butylcarbazole. The 3,5-positions were also substituted with phenyl or thienyl groups in the aza–BODIPYs. Photophysical, electrochemical, and computational studies were carried out. The absorption and emission spectra of aza–BODIPYs were significantly redshifted (≈ 100 nm) relative to the parent tetra-

phenylaza–BODIPY. Fluorescence studies suggested effective energy transfer (up to 93%) from donor groups to the aza–BODIPY core in all of the compounds under study. Time-dependent (TD)-DFT studies indicated effective electronic interactions between energy donor groups and aza–dipyrrin unit in all the aza–BODIPYs studied. The HOMO–LUMO gap (ΔE) calculated from cyclic voltammetry data was found to be lower for six aza–BODIPYs relative to their corresponding aza–dipyrrins.

Introduction

Sunlight is one of the best sources of alternative energy, and the absorption of the wide-spectrum solar energy is one of the challenges addressed by the scientists.^[1] Artificial light-harvesting antenna systems have been a matter of interest for decades and have inspired research to create better molecules for this purpose.^[2] To mimic natural light-harvesting systems like chlorophylls, many model compounds based on porphyrin or phthalocyanines have been synthesized and studied.^[3] Among these model systems, donor–acceptor (D–A)-type porphyrin–BODIPY (BF₂-chelated dipyrrromethene) conjugates are popular because selective excitation of the donor (BODIPY) is possible in such systems.^[4] BODIPYs have good photostability, a high molar absorption coefficient, and high quantum yields in the visible region.^[5] However, *meso*-aryl-substituted BODIPYs

have small Stokes shifts (10–25 nm) and narrow emission in the 520–600 nm range.^[6] Synthetic modifications such as the rigidification of difluoroboryl unit,^[7] extended aromatic conjugation,^[8] and substitution of electron-rich aromatic groups^[9] in BODIPYs have resulted in redshifted absorption and emission of such molecules. When the *meso*-carbon is replaced by a *meso*-nitrogen atom in the dipyrrromethene core, then such molecules are called aza–BODIPYs.^[5,10] The chemistry of aza–BODIPYs has seen significant growth in the last decade, and several derivatives in which the thiophene rings have occupied the 1,7- or 3,5-, or 2,6-positions of the aza–BODIPY core have been reported.^[11] Thiophene substitution, particularly at the 3,5-position of aza–BODIPYs, causes significant redshifts in their absorption and emission owing to increased conjugation in the molecule. Aza–BODIPYs have also been used as chemosensors.^[12a,e] 1,7-bis(2-pyridyl)-3,5-diphenylaza–BODIPY showed high selectivity for Hg²⁺ sensing with redshifted absorption and emission maxima.^[12b] The crown-ether-substituted aza–BODIPYs have been used as visible sensors for the detection of shellfish toxin.^[12c] Aza–BODIPYs with thiophene rings at the 1,7-positions and fluorene/*N*-methylcarbazole substituents at the 3,5-phenyl positions have been used as fluorescence sensors for Hg²⁺ ions.^[12d] The supramolecular self-assemblies of aza–BODIPY-fullerene and aza–BODIPY-zinc phthalocyanines have been successfully synthesized, and electron-transfer studies were reported by D'Souza and co-workers.^[13] Burgess and co-workers have reported fluorescein-attached aza–BODIPYs as energy-transfer cassettes and boron-chelated aza–BODIPYs.^[14] The chromophores with absorption and emission into the near-infrared (NIR) region are very much in demand for cell recognition and in vivo imaging, because deep penetration into biological tissues is possible by NIR fluorescence.^[15] Aza–

[a] N. Balsukuri, Dr. I. Gupta
Indian Institute of Technology Gandhinagar
Village Palaj, Simkheda, Gandhinagar
Gujarat-382355 (India)
E-mail: iti@iitgn.ac.in

[b] M. Y. Lone, Dr. P. C. Jha
School of Chemical Sciences
Central University of Gujarat
Gandhinagar, Gujarat (India)

[c] Dr. S. Mori
Integrated Centre for Sciences
Ehime University
Matsuyama 790-8577 (Japan)

Supporting information for this article can be found under <http://dx.doi.org/10.1002/asia.201600167>. It contains characterization data such as HRMS as well as ¹H, ¹³C, ¹⁹F, ¹¹B NMR, and fluorescence spectra. The energy and coordinates used for DFT calculations of compounds 19–24 are also included.

BODIPYs are very promising NIR chromophores that can be used in materials and biology as photosensitizers.^[16a-e] Benzanulated aza-BODIPY^[17] have been tested as photosensitizers for applications in organic solar cells. Aza-BODIPYs display significantly redshifted (≈ 100 nm) absorption and emission relative to the parent BODIPYs.

Owing to their excellent photophysical properties, aza-BODIPYs have been used for applications in photovoltaics, optoelectronics, bioimaging, and photodynamic therapy.^[18] The parent 1,3,5,7-tetraphenylaza-BODIPY (TPAB) absorbs and emits around 650 and 672 nm, respectively, and several approaches have been employed to shift the emission further into the NIR range with decent quantum yield efficiency. To make NIR-active aza-BODIPYs, several synthetic modifications (Figure 1)

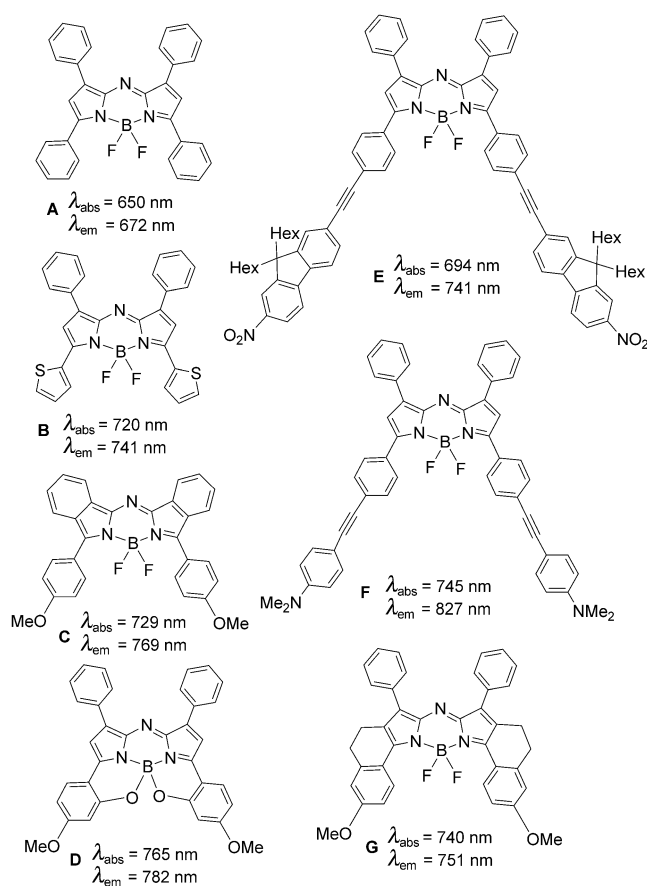


Figure 1. Selected aza-BODIPYs reported in the literature.

have been reported: extension of the π conjugation,^[19a] chelation of the boron atom by rigid aromatic groups,^[19b] attachment of donor groups onto phenyl rings,^[19c] substitution at the aza-BODIPY core by electron-withdrawing/releasing aromatic rings,^[19d] and replacement of F atoms by alkynyl/aryl groups.^[19e] In comparison to TPAB, the synthesis of such molecules involves a multistep process with lower yields, thereby limiting their applications. We were interested in creating a variety of NIR aza-BODIPYs by means of a simple straightforward synthetic method (Figure 2). In this paper, we report the syn-

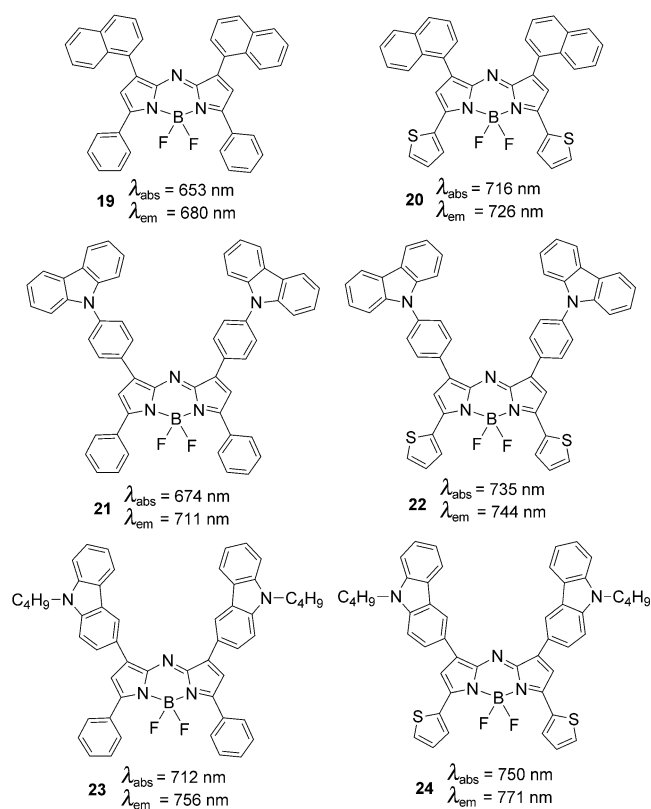


Figure 2. Donor-acceptor-type aza-BODIPYs 19-24 reported in this work (data recorded in toluene).

thesis, characterization, X-ray structure, optical, and electrochemical studies of donor-acceptor-type aza-BODIPYs. All six aza-BODIPYs exhibited redshifted emission maxima and efficient energy transfer from donor units (*N*-phenylcarbazole/*N*-butylcarbazole/naphthalene) to the acceptor unit (boron-aza-dipyrrin core). Also, computational studies were carried out to provide complementary spectroscopic insight into the six-aza-BODIPY molecules to reach semiquantitative estimates of the maximum absorption (λ_{max}) of these challenging dyes.

Results and Discussion

Synthesis and Characterization

The synthetic procedures for chalcones 1-6 and compounds 7-12 are depicted in Table 1. Chalcones 2-6 were prepared by the aldol condensation method.^[20] 2-Naphthaldehyde (1 equiv) and 2-acetylthiophene (1 equiv) were heated under reflux conditions in a mixture of methanol/water (1:1) in the presence of NaOH for two hours. The desired chalcone 2 precipitated as a yellow solid. It was purified by silica gel column chromatography using a mixture of dichloromethane (CH_2Cl_2)/hexane. Chalcone 2 was obtained in 51% yield, and chalcones 3-6 were synthesized in a similar manner. Compounds 7-12 were prepared by means of a 1,4-Michael addition reaction.^[11] Chalcone 1 (1 equiv) and nitromethane (4 equiv) were heated to reflux in a mixture of methanol/trimethylamine (3:1) for

Table 1. Synthesis of chalcones 1–6 and compounds 7–12.

R ¹	R ²	Chalcone	Compound
		1 (reported)	7 (76%)
		2 (51%)	8 (67%)
		3 (67%)	9 (63%)
		4 (72%)	10 (61%)
		5 (64%)	11 (53%)
		6 (reported)	12 (51%)

24 hours. As the reaction progressed, the color of the reaction mixture changed from yellow to black. The crude compound **7** was purified by silica gel column using a mixture of ethyl acetate/hexane in 76% yield. By following the same procedure, compounds **8–12** were synthesized in 51–67% yields.

The synthetic procedures for aza-dipyrriins and aza-BODIPYs are shown in Table 2. Aza-dipyrriins **13–18** were prepared by heating compounds **7–12** to reflux in ethanol with an excess amount of ammonium acetate for 48 hours.^[14] The resulting blue precipitate was then washed with ethanol to obtain pure aza-dipyrriins **13–18** as blue solids in 11–46% yields. Aza-dipyrin **13** (1 equiv) was treated with BF₃·OEt₂ (15 equiv) in a mixture of dry CH₂Cl₂/DIEA (diisopropylethylamine; 1:1) for 24 h under an inert atmosphere.^[14] The crude aza-BODIPY **19** was purified by silica gel column chromatography and obtained as a metallic green solid in 20% yield. Aza-BODIPYs **20–24** were also prepared in 14–30% yields by following the same procedure.

Compounds **1–24** were characterized by HRMS as well as ¹H and ¹³C NMR spectroscopy; the data are shown in the Supporting Information. Aza-BODIPYs **19–24** were also characterized by ¹⁹F and ¹¹B NMR spectroscopy (see the Supporting Information). A representative ¹H NMR and HOMO-COSY spectrum of aza-BODIPY **24** is shown in Figure 3. The characteristic β-pyrrole protons and α-thiophene protons appeared as singlets at δ = 7.16 and 8.39 ppm, respectively. The other β-thiophene proton signals appeared between δ = 7.58 and 7.25 ppm. The

Table 2. Synthesis of aza-dipyrriins **13–18** and aza-BODIPYs **19–24**.

R ¹	R ²	Aza-dipyrin	Aza-BODIPY
		13 (29%)	19 (20%)
		14 (11%)	20 (21%)
		15 (29%)	21 (15%)
		16 (18%)	22 (14%)
		17 (46%)	23 (23%)
		18 (21%)	24 (30%)

fourteen aromatic protons of the *N*-butylcarbazole ring appeared between δ = 8.83 to 7.02 ppm, and the aliphatic protons appeared as four sets of signals between δ = 4.20 to 0.90 ppm. The ¹⁹F NMR spectra of aza-BODIPYs **19–24** were recorded in CDCl₃, and the fluorine resonance signals split into quartets owing to the coupling with the adjacent boron atom (¹¹B, *I* = 3/2) and only one ¹⁹F signal was observed owing to the symmetrical nature of the molecules (Table 3).^[9] For compounds **19–24** the ¹⁹F quartet appeared between δ = –130.38 to –139.32 ppm (Table 3). The ¹¹B signals of aza-BODIPYs **19–24** appeared as triplets between δ = 1.04 to 1.47 ppm.

Interestingly, the ¹⁹F signals of 3,5-thienyl-substituted aza-BODIPYs were slightly downfield-shifted relative to the 3,5-phenyl-substituted compounds (Table 3). A similar trend was

Table 3. Chemical-shift values of heteronuclear NMR spectroscopic data recorded in CDCl₃.

Compound	¹⁹ F signal (δ) [ppm]	¹¹ B signal (δ) [ppm]
19	–131.59 (q, 2F)	1.18 (t, 1B)
20	–139.32 (q, 2F)	1.47 (t, 1B)
21	–131.18 (q, 2F)	1.04 (t, 1B)
22	–138.58 (q, 2F)	1.37 (t, 1B)
23	–130.38 (q, 2F)	1.05 (t, 1B)
24	–137.34 (q, 2F)	1.30 (t, 1B)

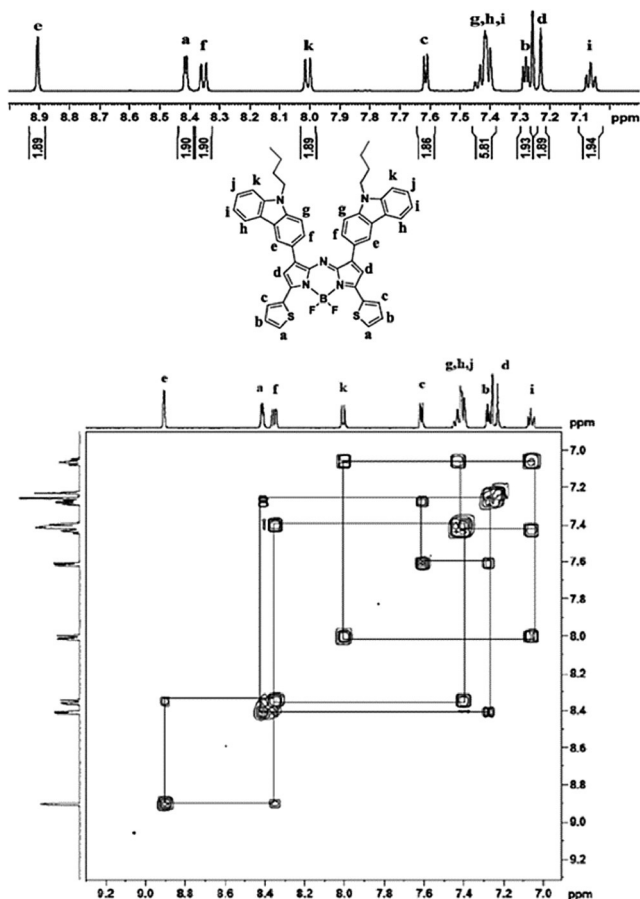


Figure 3. ^1H NMR and ^1H - ^1H COSY spectra of aza-BODIPY **24** in CDCl_3 .

observed for ^{11}B chemical shifts in aza-BODIPYs **19**–**24**, which suggests the increased delocalization of electron density in the aza-dipyrrin core of 3,5-thienyl-substituted compounds, thereby resulting in the slight downfield shifts of the ^{19}F and ^{11}B signals.

Single-Crystal X-ray Diffraction Studies

The single-crystal X-ray structures of aza-dipyrrins **13** (CCDC 1016009) and **14** (CCDC 1425995) were solved. ORTEP views of aza-dipyrrins **13** and **14** are given in Figure 4; X-ray structural parameters and selected bond lengths and bond angles are presented in Tables 4 and 5, respectively. Single crystals of compound **13** were obtained by slow evaporation of the chloroform/*n*-heptane solution over a period of one week. Aza-dipyrrin **13** gave green block crystals with a triclinic crystal system in the $P\bar{1}$ (no. 2) space group. The aza-dipyrrin core of compound **13** was essentially planar, which is similar to the reported ferrocenyl-substituted aza-dipyrrin compound.^[21] The two naphthyl units were found in *syn* conformation, and the dihedral angles ($\text{C}5\text{-C}6\text{-C}25\text{-C}34$, $\text{C}4\text{-C}3\text{-C}15\text{-C}16$) between the aza-dipyrrin core and naphthyl units were $42.4(3)$ and $42.6(3)^\circ$, respectively. The tor-

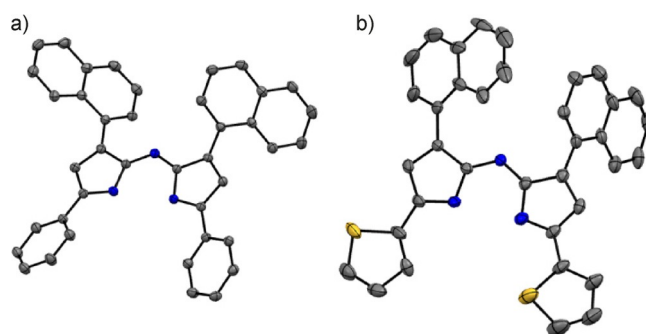


Figure 4. ORTEP diagrams of a) aza-dipyrrin **13** and b) aza-dipyrrin **14**. Thermal ellipsoids are shown at the 50% probability level (hydrogen atoms are omitted for clarity).

sion angles ($\text{N}3\text{-C}8\text{-C}35\text{-C}40$, $\text{N}1\text{-C}1\text{-C}9\text{-C}10$) between the aza-dipyrrin core and two phenyl rings were $23.3(3)$ and $22.4(3)^\circ$, respectively. These dihedral angles were higher than the reported values of the 1,7-diphenyl-3,5-diferrocenyl-aza-dipyrrin^[21] (19.81 and 21.25° , respectively). Intramolecular hydrogen bonding was observed in **13** between the $\text{N}3\text{-H-N}1$ (D-H-A) with a bond angle of 119.31° , and the hydrogen-bond length was 2.16 \AA . Single crystals of compound **14** were obtained by slow evaporation of a chloroform solution over a period of one week. Aza-dipyrrin **14** gave violet block crystals with a monoclinic crystal system in the C_2 (no. 5) space group. In compound **14** two naphthyl units were arranged in a perpendicular manner, and the dihedral angles ($\text{C}6\text{-C}7\text{-C}23\text{-C}24$, $\text{C}4\text{-C}3\text{-C}13\text{-C}14$) between the aza-dipyrrin core and naphthyl units were $43.5(6)$ and $43.0(6)^\circ$, respectively. The torsion angles ($\text{N}3\text{-C}8\text{-C}33\text{-C}34$, $\text{N}1\text{-C}1\text{-C}9\text{-C}10$) between the aza-dipyrrin core and two thienyl groups were $4.8(10)$ and $8.0(8)^\circ$, respectively. Also, the torsion angles ($\text{N}3\text{-C}8\text{-C}33\text{-S}2$, $\text{N}1\text{-C}1\text{-C}9\text{-S}1$) between the aza-dipyrrin core and two thienyl groups that involved thiophene atoms were $15.7(8)$ and $4.2(7)^\circ$, respectively. The torsion

Table 4. Crystal structure data and refinement parameters of **13** and **14**.

	Compound 13	Compound 14
Empirical formula	$\text{C}_{41}\text{H}_{28}\text{Cl}_3\text{N}_3$	$\text{C}_{36.5}\text{H}_{23.5}\text{Cl}_{1.5}\text{N}_3\text{S}_2$
Formula weight	669.05	621.41
Crystal color, habit	green, block	violet, block
Crystal dimensions [mm]	$0.250 \times 0.200 \times 0.130$	$0.200 \times 0.030 \times 0.030$
Crystal system	triclinic	monoclinic
Lattice type	primitive	C-centered
<i>a</i> [Å]	9.523(4)	27.580(10)
<i>b</i> [Å]	13.112(7)	7.565(3)
<i>c</i> [Å]	13.426(7)	13.879(5)
α [°]	103.569(9)	–
β [°]	99.317(7)	92.131(6)
γ [°]	92.669(6)	–
<i>V</i> [Å ³]	1601.9(13)	2893.8(18)
<i>Z</i>	2	4
<i>D</i> _{calcd} [g cm ⁻³]	1.387	1.426
μ [cm ⁻¹]	3.219	3.555
Goodness-of-fit on <i>F</i> ²	1.09	1.10
Reflections collected/unique	31077/9544	28459/8623
<i>R</i> (int)	0.0339	0.0466
Space group	$P\bar{1}$ (no. 2)	C_2 (no. 5)

Table 5. Comparison of selected bond lengths [Å] and bond angles [°] of **13** and **14**.

	Compound 13	Compound 14
N1–C1	1.344(3)	1.321(5)
N1–C4	1.395(3)	1.405(6)
N2–C4	1.319(3)	1.307(5)
N2–C5	1.338(3)	1.358(5)
C5–N3	1.388(3)	1.369(5)
C8–N3	1.346(3)	1.368(5)
C5–N2–C4	122.61(17)	122.3(4)
C5–C6–C7	105.77(17)	106.4(3)
N3–C5–C6	108.46(18)	108.0(3)
C5–N3–C8	108.31(17)	109.4(3)
N3–C8–C7	109.60(18)	107.7(4)
N2–C5–N3	126.04(18)	124.8(4)
N2–C4–C3	124.93(18)	124.0(4)
N1–C4–N2	126.12(19)	125.9(4)
C2–C3–C4	105.64(18)	105.2(4)
N1–C1–C2	110.69(17)	113.0(4)
C1–N1–C4	107.20(17)	105.1(3)

angles between the aza-dipyrrin core and phenyl rings (**13**) were larger with respect to the aza-dipyrrin core and thiophene ring (**14**), thus indicating better electronic interactions between smaller thiophene rings and the aza-dipyrrin core in compound **14**. Non-coplanar arrangements of naphthyl rings with regard to the aza-dipyrrin core indicated less effective electronic interactions between the two moieties in compounds **13** and **14**.

Photophysical Studies

Absorption Studies

The absorption studies of aza-dipyrrins **13–18** and aza-BODIPYs **19–24** were carried out in four different solvents that ranged from polar to nonpolar. A comparison of absorption spectra of **13–18** in CH₂Cl₂ is presented in Figure 5. Also, a comparison of absorption spectra of **19–24** is presented in Figure 6; data are given in Table 6. The absorption spectra of aza-dipyrrins **13–18** exhibited the π - π^* transitions of dipyrrin ligand^[22] with two absorption bands in the visible region. Aza-

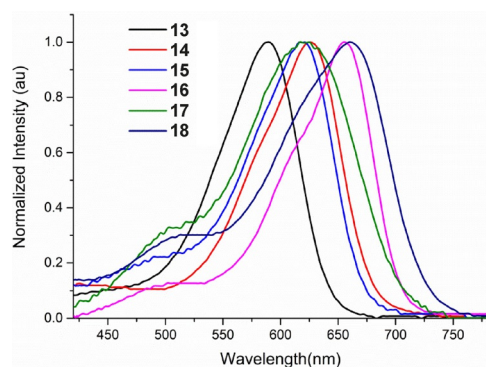


Figure 5. Comparison of the absorption spectra of aza-dipyrrins **13–18** in CH₂Cl₂.

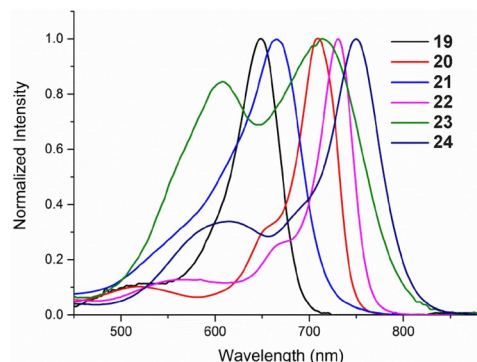


Figure 6. Comparison of the absorption spectra of aza-BODIPYs **19–24** in CH₂Cl₂.

dipyrrins **13–18** exhibited an intense absorption band in the region of 590–662 nm in toluene, which corresponded to π - π^* transitions that originated from the dipyrrin ligand. Another small absorption band appeared in the 290–345 nm range in all the dipyrrins under study. The extinction coefficients of aza-dipyrrins **13–18** were in the range of 27000 to 61000 M⁻¹cm⁻¹, values that were much lower than the corresponding aza-BODIPYs **19–24**. The UV/Vis absorption maxima of aza-dipyrrins **13–18** were dependent on the nature of substituents at the 3,5- and 1,7-positions of the dipyrrin core.^[11] For example, in compounds **13**, **15**, and **17**, the 1,7-substituents were varied from naphthyl to *N*-phenylcarbazole to *N*-butylcarbazole and 3,5-diphenyl substituents remained common to all of them. It is clear from Table 6 that moving from naphthyl (**13**) to *N*-phenylcarbazole (**15**) at the 1,7-positions resulted in a 28 nm redshift in the absorption maxima of the major absorption band, whereas only a 3 nm redshift was observed in the absorption maxima of the major absorption band upon moving from *N*-phenylcarbazole (**15**) to *N*-butylcarbazole (**17**) as 1,7-substituents. Similarly, for compounds **14**, **16**, and **18** the 3,5-dithienyl substituents were kept common and varying the 1,7-substituents from naphthyl (**14**) to *N*-butylcarbazole (**18**) resulted in a 36 nm redshift in the absorption band. Clearly, the *N*-butylcarbazole group introduced about 31–35 nm bathochromic shifts in the absorption maxima relative to naphthyl groups in aza-dipyrrins. This could be attributed to the electron-donating nature of the bulky carbazole ring in these compounds.^[9] The wavelengths of major absorption bands of 3,5-dithienyl-substituted compounds **14**, **16**, and **18** were significantly redshifted (41 to 46 nm) relative to their 3,5-diphenyl-substituted counterparts **13**, **15**, and **17** respectively. The significant bathochromic shifts were ascribed to the smaller torsion angles and higher electron-donating ability of thienyl groups versus phenyl groups within the compounds.^[12] The absorption bands of **13–18** were sharp with full width at half-maxima (fwhm_{abs}) varying from 82 to 116 nm in toluene (Table 6). Also, the absorption maxima for **13–18** were insensitive to solvent polarity and varied slightly (2–8 nm) upon changing the solvent from toluene to tetrahydrofuran. The absorption spectra of aza-BODIPYs **19–24** showed a similar pattern to their corresponding aza-dipyrrins **13–18**. The major ab-

Table 6. Absorption data of compounds **13–24** in various solvents.

Compound	Solvent	λ_{abs} [nm], ϵ (log E)	fwhm	
			[nm]	[cm^{-1}]
13	toluene	590 (4.72)	82	2458
	dichloromethane	586 (4.67)	81	2449
	chloroform	589 (4.63)	80	2397
	tetrahydrofuran	585 (4.54)	82	2492
14	toluene	626 (4.70)	84	2253
	dichloromethane	623 (4.67)	86	2315
	chloroform	625 (4.63)	86	2299
	tetrahydrofuran	621 (4.59)	86	2330
15	toluene	618 (4.42)	87	2441
	dichloromethane	613 (4.35)	88	2446
	chloroform	615 (4.32)	85	2337
	tetrahydrofuran	616 (4.29)	87	2401
16	toluene	655 (4.61)	82	1997
	dichloromethane	653 (4.57)	90	2222
	chloroform	654 (4.55)	90	2215
	tetrahydrofuran	652 (4.53)	89	2200
17	toluene	sh 501(3.93), 621 (4.38)	116	3094
	dichloromethane	sh 506 (3.84), 618 (4.30)	116	3125
	chloroform	sh 503 (3.77), 621 (4.25)	115	3082
	tetrahydrofuran	sh 502 (3.77), 616 (4.15)	130	3569
18	toluene	sh 509 (4.25), 662 (4.78)	109	2651
	dichloromethane	sh 510 (4.19), 658 (4.70)	116	2855
	chloroform	sh 514 (4.14), 661 (4.66)	113	2758
	tetrahydrofuran	sh 514 (4.02), 658 (4.53)	114	2805
19	toluene	653 (4.96)	53	1262
	dichloromethane	648 (4.91)	56	1352
	chloroform	650 (4.85)	56	1344
	tetrahydrofuran	649 (4.80)	55	1326
20	toluene	sh 654 (4.43), 716 (5.10)	38	748
	dichloromethane	sh 652 (4.41), 714 (5.06)	40	794
	chloroform	sh 653 (4.36), 716 (5.03)	40	789
	tetrahydrofuran	sh 652 (4.32), 712 (4.97)	38	756
21	toluene	674 (4.83)	71	1612
	dichloromethane	668 (4.80)	80	1871
	chloroform	670 (4.78)	76	1761
	tetrahydrofuran	670 (4.58)	74	1709
22	toluene	sh 667 (4.47), 735 (5.14)	41	766
	dichloromethane	sh 668 (4.46), 733 (5.08)	41	771
	chloroform	sh 667 (4.31), 733 (5.03)	40	751
	tetrahydrofuran	sh 669 (4.30), 731 (4.97)	39	735
23	toluene	598 (4.44), 712 (4.64)	–	–
	dichloromethane	602 (4.46), 712 (4.57)	–	–
	chloroform	606 (4.43), 711 (4.51)	–	–
	tetrahydrofuran	606 (4.25), 713 (4.35)	–	–
24	toluene	595 (4.38), 750 (4.94)	54	971
	dichloromethane	613 (4.38), 752 (4.91)	68	1224
	chloroform	601 (4.37), 750 (4.89)	60	1076
	tetrahydrofuran	606 (4.35), 748 (4.80)	67	1214

sorption band designated as the S_0 – S_1 transition was observed between 653–750 nm in aza-BODIPYs **19–24**.^[18b] In addition to this, a shoulder that corresponded to the 0–1 vibrational transition appeared in the 519 to 590 nm range for compounds **20** and **22–24**. The absorption maxima of 3,5-dithienyl-substituted compounds **20**, **22**, and **24** were significantly redshifted (38 to 63 nm in toluene) relative to their 3,5-diphenyl-substituted counterparts **19**, **21**, and **23**, respectively. This trend was consistent with the reported data of 3,5-dithienyl-substituted aza-BODIPYs.^[11] Also, by varying the 1,7-substituents from naphthyl

(**19**) to *N*-phenylcarbazole (**21**) to *N*-butylcarbazole (**23**), 21–38 nm bathochromic shifts were observed in their absorption maxima. Their absorptions were sharp with full-width at half-maxima (fwhm_{abs}) varying from 41 to 80 nm in CH_2Cl_2 (Table 6). The absorption maxima for **19–24** varied slightly (2–8 nm) upon changing the solvent polarity from nonpolar to polar; this trend was in line with the reported BODIPY chromophores.^[5a,22] The solvent polarity affected the broadening of the absorption band, and fwhm_{abs} values were lower in nonpolar solvent and slightly higher in polar solvents for compounds **19–24**.^[5a,22] The extinction coefficients of **19–24** were in the range of 63 000–140 000 $\text{M}^{-1}\text{cm}^{-1}$, which were much larger than the corresponding aza-dipyrins, thus making these dyes potentially useful for biological applications. Among the aza-BODIPYs **19–24**, a maximum redshifted absorption at 750 nm was observed for **24** (Table 6). The absorptions of aza-BODIPYs **19–24** demonstrate that simple substitution by electron-rich aromatic moieties at the 1,7-positions can lead to significant bathochromic shifts rather than making conformationally restricted aza-BODIPYs, which are difficult to synthesize.

Fluorescence Studies

Fluorescence studies of all of the aza-BODIPYs (**19–24**) were carried out in various solvents of different polarities and emission quantum yields were calculated; emission data are presented in Table 7, and emission spectra are given in Figure 7.

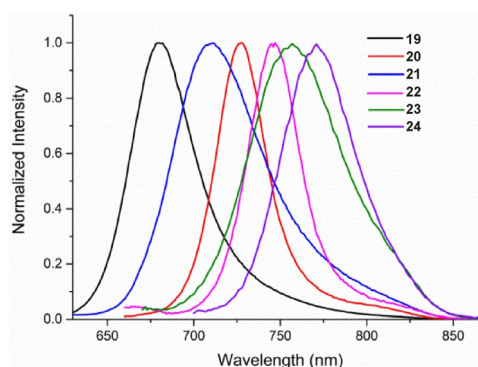


Figure 7. Comparison of the emission spectra of aza-BODIPYs **19–24** in toluene.

The typical mirror-image relationship was observed for the lowest-energy absorption band and the emission spectra of all these compounds (**19–24**).^[23] The emission maxima for compounds **19–24** were redshifted relative to that of TPAB.^[11] The emission maxima of aza-BODIPYs **19**, **21**, and **23** were compared with the corresponding TPAB in chloroform; **19** showed a small shift, whereas **21** and **23** exhibited redshifts of 49 and 102 nm, respectively (Table 7). The emission quantum yields of **21** and **23** were lower than TPAB ($\Phi_f = 0.34$, CHCl_3), whereas it was comparable with that of **19**. Similarly, the emission maxima of aza-BODIPYs **20**, **22**, and **24** were compared with the corresponding 1,7-diphenyl-3,5-dithienylaza-BODIPY in chloroform;^[11] compound **20** showed a 12 nm blueshift, where-

Table 7. Emission data of aza-BODIPYs **19–24** in different solvents.

Compound	Solvent	λ_{em} [nm]	$\Phi_f^{[a]}$	fwhm [nm]	Stokes shift		
					[cm^{-1}]	[nm]	[cm^{-1}]
19	toluene	680	0.47 ^[b]	45	967	27	608
	dichloromethane	682	0.25	49	1053	34	769
	chloroform	681	0.36	46	987	31	700
	tetrahydrofuran	677	0.25	46	995	28	637
20	toluene	726	0.14	35	616	10	192
	dichloromethane	728	0.13	35	665	14	269
	chloroform	729	0.13	36	679	13	249
	tetrahydrofuran	723	0.11	35	770	11	213
21	toluene	711	0.31	61	1197	37	772
	dichloromethane	743	0.01	84	1522	75	1511
	chloroform	721	0.14	94	1761	51	1055
	tetrahydrofuran	710	0.01	56	1154	40	840
22	toluene	744	0.09	37	666	9	164
	dichloromethane	745	0.02	39	702	12	219
	chloroform	744	0.09	37	666	11	201
	tetrahydrofuran	743	0.03	36	652	12	220
23	toluene	756	0.04	64	1112	44	817
	dichloromethane	797	0.01	77	1228	85	1497
	chloroform	774	0.02	79	1306	63	1144
	tetrahydrofuran	784	0.01	81	1316	71	1270
24	toluene	771	0.04	53	889	21	363
	dichloromethane	795	0.01	74	1179	45	754
	chloroform	779	0.02	68	1108	29	496
	tetrahydrofuran	785	0.01	73	1179	37	630

[a] Zinc-phthalocyanine ($\Phi_f=0.30$, toluene) used as standard, $\lambda_{ex}=650$ nm. [b] TPAB ($\Phi_f=0.34$, chloroform) used as standard, $\lambda_{ex}=610$ nm.

as **22** and **24** exhibited redshifts of 3 and 30 nm, respectively (Table 7). The emission quantum yields of **20**, **22**, and **24** were lower than the corresponding aza-BODIPY ($\Phi_f=0.44$, toluene). Among the three donor groups at the 1,7-positions of aza-BODIPYs **19–24**, the naphthyl rings clearly had no or little effect on the emission maxima of **19** and **20**. However, *N*-phenylcarbazole and *N*-butylcarbazole groups influenced 38–99 nm bathochromic shifts in the emission maxima of **21–24**; maximum redshifts occurred in compounds **23** and **24** with 1,7-*N*-butylcarbazole groups. Solvatochromic studies revealed that aza-BODIPYs **19**, **20**, and **22** showed small shifts (2–6 nm) in emission maxima by changing the polarity of the solvents (Table 7), whereas changing the solvent polarity resulted in significant shifts (16–30 nm) in the emission maxima for aza-BODIPYs **21**, **23**, and **24**. The observed Stokes shifts for compounds **19–24** were smaller (9 to 44 nm) in nonpolar solvents and higher (34 to 85 nm) in polar solvents (Table 7). Except for compounds **20** and **22**, the rest of the aza-BODIPYs showed much higher (34–45 nm) Stokes shifts than the parent TPAB compound (22 nm in CH_2Cl_2). In polar solvents, the redshifted emission maxima reflect larger dipoles of the charge-transfer (CT) excited states, which was in agreement with the report by Boens et al.^[22] The quantum yields of aza-BODIPYs **19–24** were higher in nonpolar solvents (i.e., toluene) and lower in polar solvents (i.e., tetrahydrofuran); this is due to the large dipole moment difference between the CT excited state and the ground state, which in turn facilitate internal conversion in polar media.^[22]

Energy-transfer studies of aza-BODIPYs **19–24** were carried out in toluene. Since the aza-BODIPY core absorbs around

550–700 nm, it can act as acceptor unit and three aromatic moieties (naphthalene, *N*-phenylcarbazole, and *N*-butylcarbazole) can act as donor units. An energy transfer from donor moieties to the aza-BODIPY core was expected. Indeed, all of the compounds (**19–24**) exhibited the energy-transfer phenomenon from donor units to the aza-BODIPY core (see the Supporting Information). A comparison of emission spectra of aza-BODIPY **24** and a 2:1 mixture of *N*-butylcarbazole and TPAB is shown in Figure 8. In this system, the *N*-butylcarbazole unit acts as an energy donor and the aza-BODIPY core acts as an energy acceptor. Therefore, upon excitation of *N*-butylcarbazole unit at 320 nm in compound **24**, the dominant emission was observed from the aza-BODIPY core in the range of 740–890 nm. The free *N*-butylcarbazole molecule emits in the

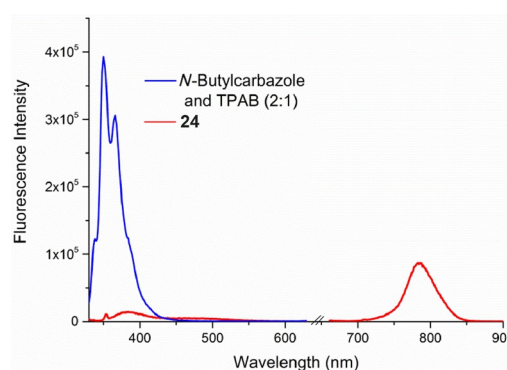


Figure 8. Comparison of the normalized emission spectra of aza-BODIPY **24** in a 2:1 mixture of corresponding monomers in toluene ($\lambda_{ex}=320$ nm).

range of 340–450 nm. It is very clear from Figure 8 that upon excitation of a 2:1 mixture of *N*-butylcarbazole and TPAB at 320 nm, the point at which *N*-butylcarbazole absorbs strongly, emission was observed exclusively from the *N*-butylcarbazole molecule around 340–368 nm and no emission was observed from TPAB. However, in the case of aza-BODIPY **24**, the excitation of the *N*-butylcarbazole unit at 320 nm resulted in the major emission from the aza-BODIPY core around 771 nm and the emission from *N*-butylcarbazole units was drastically quenched (Figure 8). The energy-transfer efficiency (ETE [%]) is a measure of total energy transfer from donor to acceptor irrespective of the mechanism and it can be calculated by the formula mentioned below.^[24] The quantum yields of the aza-BODIPY unit in all the compounds (**19–24**) were calculated at two different wavelengths, that is, excited at the donor (where the donor absorbs strongly) and excited at the acceptor (aza-BODIPY core). The data are presented in Table 8. ETE gives an idea of the extent of energy transfer including the loss in energy by non-radiative decays during the energy-transfer process.^[24] The calculated values of ETE were in the range of 70% (in **19**) to 93% (in **22**), thus indicating efficient energy transfer from donor units to acceptor units in all the compounds (Table 8). X-ray crystal structures of the key precursors (**13** and **14**) of aza-BODIPYs (**19** and **20**, respectively) showed that naphthyl moieties (donor) and the aza-dipyrrin core (acceptor) were not coplanar, therefore the possibility of energy transfer through other mechanisms is not very favorable. However, more detailed photophysical and electrochemical studies will be required to understand the mechanism of energy transfer in these compounds.

Computational Methodology

Among the whole panel of synthesized molecules, theoretical attention was paid to aza-BODIPY moieties because of their absorbance in the near-infrared region. All the simulations of aza-BODIPY derivatives (**19–24**) were accomplished with the Gaussian 09 program package^[25] Geometry optimization was carried out without symmetry constraints at the PBEPBE/6-

311G(2d,p) level of approximation.^[26] Vibrational spectra were determined analytically at the same level of theory to make sure that the given structure is at its true energy minima. Vertical linear-response TD-DFT approximation^[27] was employed to calculate electronic transition energies at the TD-BMK/6-311+G(2d,p) level of theory.^[28] The effect of dichloromethane was systematically modeled for all the steps by means of the conductor-like polarizable continuum model (C-PCM).^[29] The choice of functional and basis set was made from the TD-DFT benchmarking of aza-BODIPYs.^[30]

Geometrical Parameters

Structural parameters obtained as a result of geometry optimization at the PBEPBE/6-311G(2d,p) level of approximation was taken into consideration, and different conclusions may be drawn by scrutinizing the data. The choice of functional and basis set was made from the literature^[31] as it yields the smallest mean absolute errors for bond lengths and valence angles. Although the crystal data for the molecules of interest is not yet available, calculated results for all the dye molecules in terms of structural parameters are incorporated into Tables 9 and 10. Owing to solid-state effects, the experimental structures cannot be visualized perfectly of C_2 symmetry, therefore the average measured structural parameters for the two halves of the molecule are taken into account. The designation of bond lengths and valence angles can be seen in Figure 9. It is clear from the calculated results that the effect of substitution on the geometrical parameters of the aza-BODIPY core is negligible. To be more precise, the utmost deviation shown in terms of bond lengths and valence angles is 0.01 Å and 0.91°, respectively. These marginal deviations echo the strong influence of substitution on the absorption properties.

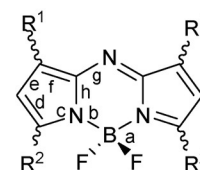


Figure 9. Representation of essential structural parameters in terms of bond lengths and valence angles of aza-BODIPY molecules.

Compound	Excitation (λ_{ex}) [nm]	Emission (λ_{em}) [nm]	Donor [ϕ_d]	Acceptor [ϕ_a]	ETE ^[a] [%]
Zn-phthalocyanine ^[a]	650	675, 741	–	0.30	–
TPAB ^[b]	610	673	–	0.34	–
19	610	680	–	0.47	70
	290	679	–	0.33	
20	650	726	–	0.14	88
	290	727	–	0.13	
21	650	711	–	0.31	81
	320	388, 709	–	0.25	
22	650	744	–	0.09	93
	320	393, 746	–	0.09	
23	650	756	–	0.04	84
	320	400, 755	–	0.03	
24	650	771	–	0.04	92
	320	771	–	0.03	

[a] ETE [%] = $\frac{\phi_a \text{ of acceptor in the molecule excited at the donor}}{\phi_a \text{ of acceptor in the molecule excited at the acceptor}} \times 100$

Table 9. Structural parameters computed at the PBEPBE/6-311G(2d,p) level of approximation.

Results	Aza-BODIPY	Bond lengths [Å] ^[a]							
		a	b	c	d	e	f	g	h
Theoretical	19	1.40	1.57	1.37	1.42	1.39	1.44	1.32	1.40
	20	1.40	1.56	1.37	1.42	1.39	1.44	1.33	1.39
	21	1.40	1.57	1.37	1.42	1.39	1.44	1.32	1.40
	22	1.40	1.57	1.37	1.42	1.39	1.44	1.33	1.39
	23	1.40	1.56	1.37	1.41	1.40	1.45	1.33	1.40
	24	1.40	1.56	1.37	1.42	1.39	1.44	1.33	1.40

[a] See Figure 9 for the identification of the bond lengths.

Table 10. Structural parameters computed at the PBEPBE/6-311G(2d,p) level of approximation.

Results	Aza-BODIPY	Valance angles [°]		
		αFBF	αBNC	αNCN
Theoretical	19	110.03	121.98	124.56
	20	110.54	122.39	124.47
	21	110.94	122.02	124.25
	22	110.56	122.32	124.21
	23	110.55	122.10	124.10
	24	110.20	122.37	124.03

Table 11. Comparison between theoretical and experimental λ_{\max} [nm]. PCM-TD-BMK/6-311+G(2d,p)//PCM-PBEPBE/6-311G(2d,p) level of approximation was employed to calculate the theoretical values.

Aza-BODIPY	19	20	21	22	23	24
Theoretical λ_{\max}	614	672	647	692	676	705
Oscillatory strength (<i>f</i>)	0.95	0.94	0.84	0.88	0.96	1.10
Experimental λ_{\max}	648	714	668	733	712	750

Absorption Spectra Studies

Theoretical simulations are often viewed as an efficient means to offer complementary spectroscopic insight. For this purpose, singlet-singlet transitions of aza-BODIPY dyes **19–24** were simulated at the PCM-TD-BMK/6-311+G(2d,p)//PCM-PBEPBE/6-311G(2d,p) level of approximation to achieve semi-quantitative estimates of the λ_{\max} of these challenging dyes. Out of the experimentally explored solvents, only CH₂Cl₂ was modeled for simulations, as solvent polarities did not show any significant shift in the absorption maxima. Before comparing the experimental and theoretical lowest-energy transitions (λ_{\max}) of the candidate dye molecules, it is better to analyze the nature of these transitions.

This was done by determining the topologies of the Kohn-Sham orbitals involved in the transitions. The frontier molecular orbitals (FMOs) for the molecules of interest (**19–24**) can be found in Figure 10 and the maximum wavelength absorption (λ_{\max}) in Table 11. For molecules **19**, **20**, **22**, **23**, and **24** the λ_{\max} is exclusively HOMO to LUMO electronic promotion, and for **21** it is an amalgam of HOMO to LUMO and HOMO-2 to LUMO with dominance of the former. The significant electronic conjugation between the aza-BODIPY core and the arms is responsible for the delocalization of the FMOs. It is evident from Figure 9 that the absorption of aza-BODIPY (**19–24**) corresponds to charge transfer from the arms to the central core.

In addition, there is also a significant overlap observed between the occupied and virtual orbitals. It

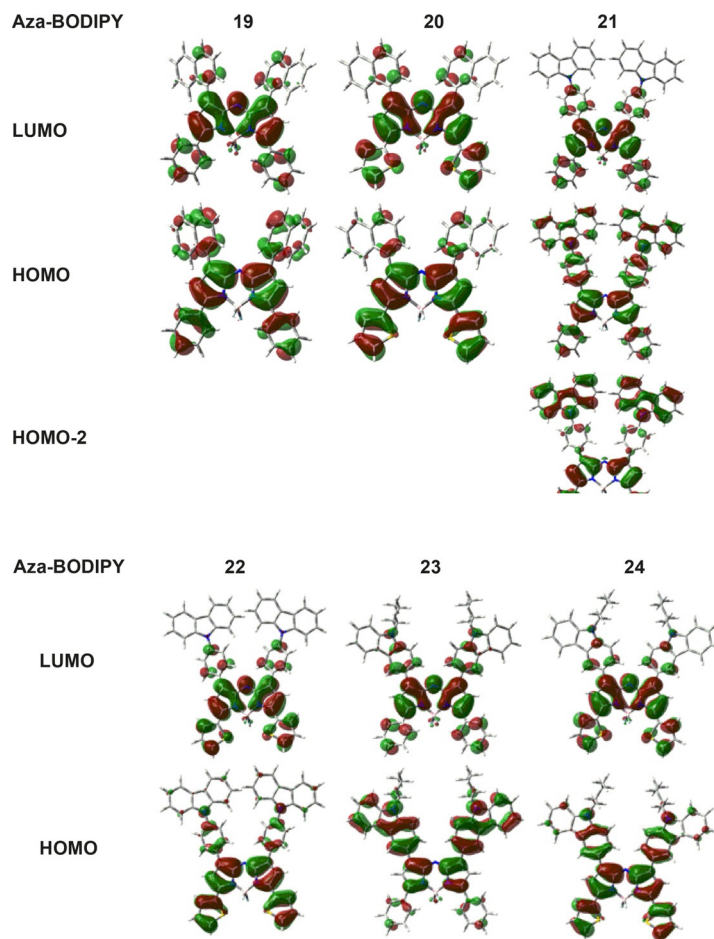


Figure 10. Six molecular orbitals for aza-BODIPYs (**19–24**) obtained at the PCM-TD-BMK/6-311+G(2d,p) level of approximation.

is apparent from the similar topologies of the LUMO of the candidate dyes (19–24) that the aza-BODIPY core acts as a strong accepting group, which suggests that the addition of an additional electron-accepting moiety is not ideal for inducing large charge transfer. Although a number of absorption bands were observed in the dye molecules (19–24), the peaks that corresponded to the lowest-energy transition (λ_{max}) were selected for comparison. The λ_{max} values of aza-BODIPY molecules 19–24 are summarized in Table 11. The experimentally obtained λ_{max} values of 20, 22, 23, and 24 are above 700 nm, and for 19 and 21 they are at 648 and 668 nm, respectively. These absorptions reflect the HOMO–LUMO gap, which is also supported by DFT studies. Although a similar trend for band-gap increments is followed, discrepancies are observed from the experimental values. To be more precise, the maximum deviation obtained is 45 nm for 24, and the minimum deviation obtained is 21 nm for 21. The consistent underestimation of λ_{max} for all the molecules is due to the inherent limitations of vertical approximation.

Electrochemical Studies

The redox potentials of compounds 13–24 were recorded in dry CH_2Cl_2 at a scan rate of 50 mVs^{-1} using 0.1 M tetrabutylammonium perchlorate (TBAP) as supporting electrolyte under N_2 atmosphere. The redox potential data and comparison of reduction waves are shown in Table 12 and Figure 11, respectively. Unlike ferrocene, which showed only one oxidation wave at 0.38 V,^[31] compounds 13–18 showed one reversible and one irreversible oxidation wave in their cyclic voltammograms (CV). Also, compounds 13–18 exhibited three reversible reduction waves between -0.38 to -1.35 V in the CVs. Compounds 19–24 exhibited two oxidation and two reduction waves in the cyclic voltammograms. Compound 19 showed one reversible and one irreversible oxidation potential in the CV; however, two irreversible oxidation waves were observed for compounds 20–22. One quasi-reversible oxidation and one irreversible oxidation wave were observed for compounds 23 and 24. In the range of -0.36 to -1.28 V , two reversible reduction

waves were observed for compounds 19–24 in the CVs. Among aza-dipyrrins, the naphthyl-substituted aza-dipyrrins 13 and 14 showed the lowest oxidation potentials (Table 12). The reduction potentials of aza-dipyrrin 15–18 (with *N*-phenylcarbazole and *N*-butylcarbazole groups) were comparatively higher than 13 and 14 (with naphthyl groups), thus making them difficult to be reduced relative to the latter. Compounds 19–24 showed two reduction waves, the first around -0.36 to -0.53 V and the second around -1.04 to -1.28 V . Compounds 19–24 showed two oxidation waves, the first around 0.68 to 1.09 V and the second around 1.32 to 1.36 V. The oxidation potential of aza-BODIPYs followed a similar trend, which was observed with aza-dipyrrins 13–14. The naphthyl-substituted aza-BODIPYs 19 and 20 showed the lowest oxidation potentials among the group. The oxidation potential values of aza-BODIPYs 19–24 were higher than those of aza-dipyrrins 13–18, thus indicating that aza-BODIPYs 19–24 were difficult to oxidize. Owing to difluoroboron (BF_2) complexation, aza-BODIPYs 19–24 became electron deficient, and the oxidation values were shifted higher. This suggests that the reduction process was more feasible for aza-BODIPYs 19–24 than aza-dipyrrins 13–18.^[11] The HOMO–LUMO energies were determined by using the measured redox potentials with the potential of Fc/Fc^+ as reference energy; they are listed in Table 12.^[32] The obtained frontier orbital energies for 13–18 and 19–24 are shown in Figures 12 and 13, respectively. The energetic stabilization for the LUMO was comparatively higher in aza-BODIPYs 19–24 than their corresponding aza-dipyrrins 13–18. The increased stabilization of the LUMO was attributed to the complexation with the BF_2 moiety in aza-BODIPYs 19–24. On comparing the effect of the substituent at the 1,7-position in compounds 13–24, it was observed that the LUMO of compounds with *N*-phenylcarbazole groups (15, 16, 21, and 22) were slightly more stabilized than the others. The data given in Table 12 clearly indicate that the energies of the HOMO were slightly higher for aza-BODIPYs 19–24 than those of the corresponding aza-dipyrrins 13–18. The HOMO–LUMO gaps (ΔE) for aza-BODIPYs 19–24 were smaller than those of the corresponding aza-dipyrrins 13–18, which is supported by the

Table 12. Electrochemical redox data (V versus SCE) of compounds 13–24 in CH_2Cl_2 that contained 0.1 M TBAP as supporting electrolyte recorded at 50 mVs^{-1} scan speed and energy levels calculated from optical and CV data.

Compound	$E_{1/2}(\text{ox})$ [V]		$E_{1/2}(\text{red})$ [V]			HOMO [eV]	LUMO [eV]	ΔE [eV] (from CV)	Optical ΔE [eV]
	I	II	I	II	III				
ferrocene	0.38	–	–	–	–	–	–	–	–
13	0.71	1.29	–0.55	–0.85	–1.24	–5.13	–3.87	1.26	1.94
14	0.77	1.33	–0.59	–0.84	–1.29	–5.19	–3.83	1.36	1.83
15	1.03	1.26	–0.38	–0.77	–1.18	–5.45	–4.04	1.41	1.85
16	0.93	1.27	–0.42	–0.74	–1.20	–5.35	–4.00	1.35	1.76
17	0.94	1.29	–0.42	–0.87	–1.33	–5.36	–3.84	1.52	1.76
18	0.99	1.33	–0.47	–0.86	–1.35	–5.41	–3.74	1.67	1.71
19	0.76	1.32	–0.50	–	–1.15	–5.09	–3.92	1.17	1.74
20	0.68	1.35	–0.42	–	–1.17	–5.11	–4.00	1.11	1.66
21	1.09	1.34	–0.37	–	–1.09	–5.35	–4.05	1.30	1.73
22	1.03	1.35	–0.36	–	–1.04	–5.30	–4.06	1.24	1.62
23	0.97	1.32	–0.53	–	–1.28	–5.37	–3.89	1.48	1.56
24	1.02	1.36	–0.48	–	–1.25	–5.44	–3.94	1.50	1.54

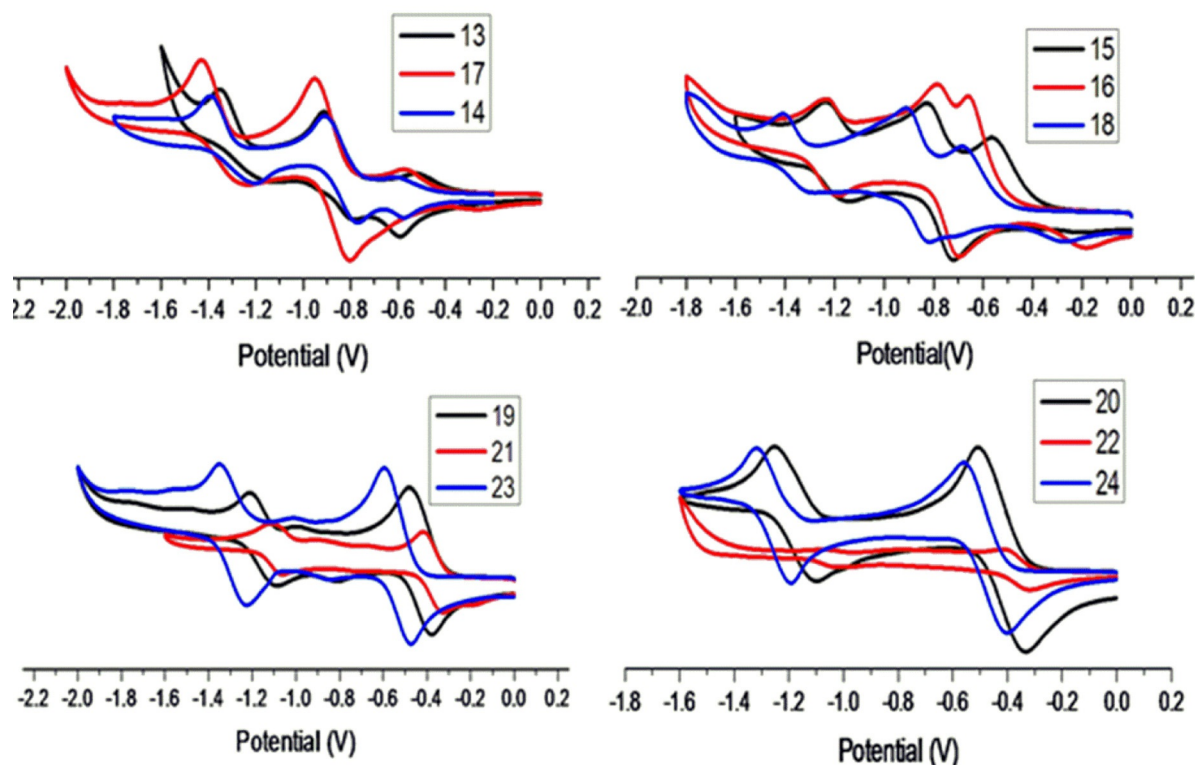


Figure 11. Comparison of the reduction waves of 13–24 in CH_2Cl_2 containing 0.1 M TBAP as a supporting electrolyte. Recorded at 50 mV s^{-1} scan speed (V versus SCE).

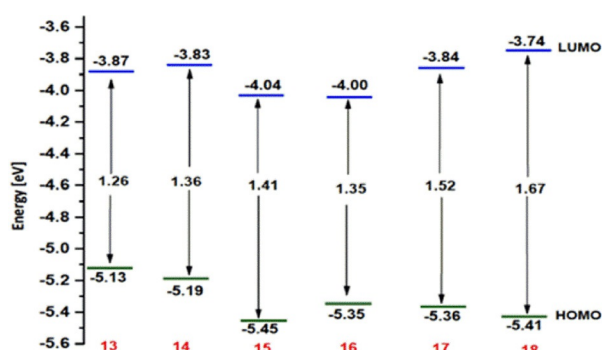


Figure 12. HOMO-LUMO energy levels of aza-dipyrins 13–18 calculated from CV data.

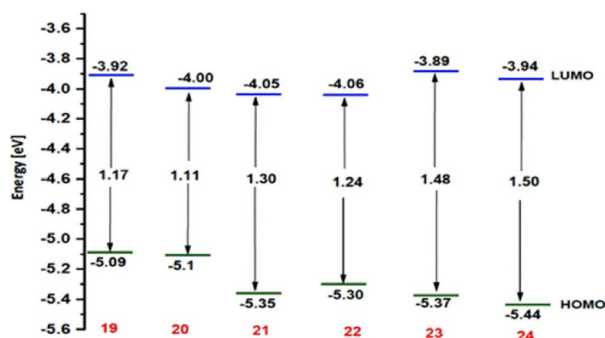


Figure 13. HOMO-LUMO energy levels of aza-BODIPYs 19–24 calculated from CV data.

trend observed in their optical properties. The absorption maxima of aza-BODIPYs 19–24 were redshifted relative to their corresponding aza-dipyrins 13–18. The electrical gaps of compounds 13–24, which were obtained from CV measurements, do not correlate with the observed absorption properties. According to electrochemical data, compounds 14 (among the aza-dipyrins) and 20 (among the aza-BODIPYs) should have the most redshifted absorption if one assumes a pure HOMO-LUMO transition. However, this is not the case, and these electrochemical studies confirm that no pure HOMO-LUMO transitions are present in the absorption process. The optical bandgap was also calculated for compounds 13–24 from the absorption data (Table 12).^[33] Among the three donor groups at the 1,7-positions of compounds 13–24, the naphthyl-substituted compounds (13, 14, 19, and 20) exhibited higher optical bandgaps than the other compounds. The lowest optical bandgap was found to be 1.54 eV for compound 24, which showed the maximum redshifted absorption among all the aza-BODIPYs, thus indicating that the *N*-butylcarbazole moiety has the maximum effect on the electronic spectra of these compounds.

Conclusion

In summary, we have described the synthesis of NIR aza-BODIPYs and aza-dipyrins that contain energy-donor groups (e.g., *N*-butylcarbazole, *N*-phenylcarbazole, naphthyl) at their 1,7-positions. Also, the 3,5-positions of the aza-BODIPYs were substi-

tuted with phenyl or thienyl groups. Fluorescence studies indicated efficient energy transfer from the donor moieties to the aza-BODIPY core in all the compounds studied. Compared to the parent TPAB, significant bathochromic shifts were observed in the optical spectra of all compounds owing to the presence of donor moieties. Furthermore, the presence of thienyl groups resulted in better electronic interactions between the aza-BODIPY core and thiophene rings, which in turn caused redshifts in the electronic spectra of such compounds relative to their 3,5-phenyl counterparts. DFT studies indicated effective electronic interactions between the donor and acceptor moieties in all the compounds under study. Electrochemical studies showed lower HOMO-LUMO gaps (ΔE) for aza-BODIPYs relative to the corresponding aza-dipyrrins owing to boron complexation. With this work we demonstrated that simple substitution with energy-donor groups on aza-BODIPYs can induce large redshifts in their electronic spectra, and this could be another strategy to create NIR dyes.

Experimental Section

Instrumentation and Reagents

Unless otherwise mentioned, all the reagents and solvents were purchased from Aldrich, Acros Organics, or Merck and used without further purification. Solvents such as dichloromethane (CH_2Cl_2) and diisopropylethylamine (DIEA) were dried as per the standard procedure. Silica gel (60–120 mesh size) used for column chromatography was procured from Merck. The NMR spectra of compounds were recorded using a Bruker Avance III 500 MHz NMR spectrometer at IIT Gandhinagar. The HRMS data for all the compounds were recorded (in positive ion mode) using a Waters Synapt-G2S ESI-Q-TOF Mass instrument at IIT Gandhinagar. Absorption spectra were recorded using a Shimadzu UV-1700. Cyclic voltammetry (CV) studies were carried out with an electrochemical system (CH1660E, CH instruments, USA) that utilized a three-electrode configuration that consisted of a glassy carbon (working electrode), platinum wire (auxiliary electrode), and saturated calomel electrode (SCE; reference electrode). The experiments were carried out under nitrogen atmosphere in dry CH_2Cl_2 using 0.1 M tetrabutylammonium perchlorate as supporting electrolyte at IIT Gandhinagar. All potentials were calibrated versus SCE by the addition of ferrocene as an internal standard with $E_{1/2}(\text{Fc}/\text{Fc}^+) = 0.38 \text{ V}$ versus SCE

General Procedure for Chalcones 1–6

A mixture of aromatic aldehyde (1 equiv) and acetophenone (1 equiv) or 2-acetylthiophene (1 equiv) was dissolved in methanol/water (1:1). After five minutes, NaOH (0.1 equiv) was added, and the reaction mixture was heated to reflux for 2 h. During the course of the reaction, the product precipitated as a yellow solid. Then the reaction mixture was extracted with CH_2Cl_2 and dried over anhydrous Na_2SO_4 . The solvent was evaporated by using a rotary evaporator under reduced pressure. The crude product was subjected to silica gel column chromatography for purification.

Compound 1: Compound 1 was prepared per the reported procedure.^[20a]

Compound 2: 1-Naphthaldehyde (4.00 g, 3.47 mL, 25.61 mmol), 2-acetylthiophene (2.76 mL, 25.61 mmol), and NaOH (0.10 g) were re-

acted in a mixture of methanol (28.00 mL)/water (28.00 mL) per the general procedure. The desired product **2** was purified by silica gel column using 45% CH_2Cl_2 /hexane as the solvent mixture. Yellow solid, yield: 3.42 g (50%); $R_f = 0.23$ (silica, CH_2Cl_2 /hexane 1:3); $^1\text{H NMR}$ (CDCl_3 , 500 MHz): $\delta = 8.6$ (d, $J = 15.5$ Hz, 1H), 8.23 (d, $J = 8$ Hz, 1H), 7.84–7.89 (m, 1H), 7.66 (d, $J = 5$ Hz, 1H), 7.55 (m, 1H), 7.46–7.52 (m, 3H), 7.15 ppm (m, 4H); $^{13}\text{C NMR}$ (CDCl_3 , 125 MHz): $\delta = 181.93$, 145.56, 140.98, 134.06, 133.78, 132.2, 132.02, 131.81, 130.92, 128.8, 128.36, 127.05, 126.37, 125.47, 125.15, 124.32, 123.54 ppm; HRMS (ESI-Q-TOF): m/z calcd for $\text{C}_{17}\text{H}_{13}\text{OS}^+$: 265.0687 $[\text{M}+\text{H}]^+$; found: 265.0706.

Compound 3: *N*-Phenylcarbazole aldehyde (1.00 g, 3.68 mmol), acetophenone (0.43 mL, 3.68 mmol), and NaOH (0.015 g) were reacted in a mixture of methanol (4.00 mL)/water (4.00 mL) by following the general procedure. The crude product **3** was purified by silica gel column using 45% CH_2Cl_2 /hexane as the solvent mixture. Yellow solid, yield: 0.66 g (48%); $R_f = 0.21$ (silica, CH_2Cl_2 /hexane 1:1.5); $^1\text{H NMR}$ (CDCl_3 , 500 MHz): $\delta = 8.15$ (d, $J = 7.5$ Hz, 2H), 8.07 (d, $J = 7$ Hz, 2H), 7.87–7.93 (m, 3H), 7.65 (m, 3H), 7.61 (m, 1H), 7.54 (m, 2H), 7.48 (d, $J = 8.5$ Hz, 2H), 7.42 (m, 2H), 7.31 ppm (m, 2H); $^{13}\text{C NMR}$ (CDCl_3 , 125 MHz): $\delta = 190.35$, 143.64, 140.45, 139.71, 138.18, 133.76, 132.95, 129.93, 128.73, 128.56, 127.19, 126.14, 123.71, 122.58, 120.44, 120.41, 109.8 ppm; HRMS (ESI-Q-TOF): m/z calcd for $\text{C}_{27}\text{H}_{20}\text{NO}^+$: 374.1545 $[\text{M}+\text{H}]^+$; found: 374.1538.

Compound 4: *N*-Phenylcarbazole aldehyde (1.00 g, 3.68 mmol), 2-acetylthiophene (0.39 mL, 3.68 mmol), and NaOH (0.015 g) were reacted in a mixture of methanol (4.00 mL)/water (4.00 mL). The crude product **4** was purified by column chromatography on silica gel using 45% CH_2Cl_2 /hexane as the solvent mixture. Yellow solid, yield: 0.76 g (54%); $R_f = 0.22$ (silica, CH_2Cl_2 /hexane 1:1); $^1\text{H NMR}$ (CDCl_3 , 500 MHz): $\delta = 8.14$ (d, $J = 8$ Hz, 2H), 7.90–7.95 (m, 2H), 7.86 (d, $J = 8.5$ Hz, 2H), 7.69 (d, $J = 4.5$ Hz, 1H), 7.64 (d, $J = 8.5$ Hz, 2H), 7.46–7.50 (m, 3H), 7.41 (m, 2H), 7.30 (t, $J = 7.5$ Hz, 2H), 7.19–7.24 ppm (m, 1H); $^{13}\text{C NMR}$ (CDCl_3 , 125 MHz): $\delta = 181.85$, 145.52, 142.90, 140.44, 139.76, 134.10, 133.56, 131.93, 129.98, 128.35, 127.16, 126.16, 123.72, 122.15, 120.46, 120.43, 109.82 ppm; HRMS (ESI-Q-TOF): m/z calcd for $\text{C}_{25}\text{H}_{18}\text{NOS}^+$: 380.1109 $[\text{M}+\text{H}]^+$; found: 380.1111.

Compound 5: *N*-Butylcarbazole aldehyde (2.00 g, 7.95 mmol), acetophenone (0.93 mL, 7.95 mmol), and NaOH (0.03 g) were reacted in a mixture of methanol (8.64 mL)/water (8.64 mL). The crude product **5** was purified by column chromatography on silica gel using a 40% CH_2Cl_2 /hexane mixture. Yellow solid, yield: 1.79 g (63%); $R_f = 0.24$ (silica, CH_2Cl_2 /hexane 1:2); $^1\text{H NMR}$ (CDCl_3 , 500 MHz): $\delta = 8.35$ (s, 1H), 8.12 (d, $J = 8$ Hz, 2H), 8.03–8.07 (m, 3H), 7.77 (d, $J = 8.5$ Hz, 1H), 7.57 (m, 2H), 7.47–7.52 (m, 3H), 7.40 (m, 2H), 7.27 (m, 1H), 4.29 (t, $J = 7.5$, 2H), 1.82–1.88 (m, 2H), 1.35–1.43 (m, 2H), 0.94 ppm (m, 3H); $^{13}\text{C NMR}$ (CDCl_3 , 125 MHz): $\delta = 190.72$, 146.57, 142.03, 141.01, 138.87, 132.42, 128.57, 128.47, 126.33, 125.92, 123.41, 122.79, 121.60, 120.60, 119.71, 119.14, 109.18, 109.17, 43.08, 31.12, 20.55, 13.87 ppm; HRMS (ESI-Q-TOF): m/z calcd for $\text{C}_{25}\text{H}_{24}\text{NO}^+$: 354.1858 $[\text{M}+\text{H}]^+$; found: 354.1835.

Compound 6: *N*-Butylcarbazole aldehyde (3.00 g, 11.93 mmol), 2-acetylthiophene (1.28 mL, 11.93 mmol), and NaOH (0.05 g) were reacted in a mixture of methanol (13.00 mL)/water (13.00 mL). The crude product **6** was purified by silica gel column using a 40% CH_2Cl_2 /hexane mixture. Yellow solid, yield: 2.52 g (58%); $R_f = 0.19$ (silica, CH_2Cl_2 /hexane 1:3); $^1\text{H NMR}$ (CDCl_3 , 500 MHz): $\delta = 8.35$ (s, 1H), 8.13 (d, $J = 7.5$ Hz, 2H), 8.08 (d, $J = 15.5$ Hz, 1H), 7.90 (d, $J = 3.5$ Hz, 1H), 7.76 (d, $J = 8.5$ Hz, 1H), 7.65 (d, $J = 4.5$ Hz, 1H), 7.45–7.50 (m, 2H), 7.40 (m, 2H), 7.28 (d, $J = 7.5$ Hz, 1H), 7.18 (m, 1H), 4.29 (m, 2H), 1.85 (q, $J = 7.5$ Hz, 2H), 1.36–1.43 (m, 2H), 0.94 ppm (m, 3H); $^{13}\text{C NMR}$ (CDCl_3 , 125 MHz): $\delta = 182.16$, 146.13, 145.72,

142.05, 141.00, 133.27, 131.33, 128.17, 126.37, 126.35, 125.72, 123.4, 122.78, 121.65, 120.61, 119.73, 118.53, 109.19, 109.17, 43.07, 31.12, 20.55, 13.88 ppm; HRMS (ESI-Q-TOF): m/z calcd for $C_{23}H_{22}NOS^+$: 360.1422 $[M+H]^+$; found: 360.1420.

General Procedure for Compounds 7–12

A chalcone (1 equiv) was dissolved in a mixture of methanol/triethylamine (Et_3N ; 3:1). After 5 min, nitromethane (4 equiv) was added into the reaction flask. Then the reaction mixture was heated to reflux for 24 h. As the reaction progressed, the color changed from light yellow to black. The reaction mixture was extracted with ethyl acetate and dried over anhydrous Na_2SO_4 . The solvent was evaporated by using a rotary evaporator under reduced pressure. The desired product was subjected to silica gel column chromatography for purification.

Compound 7: Chalcone **1** (2.00 g, 7.74 mmol) and nitromethane (1.65 mL, 30.96 mmol) were reacted in a mixture of methanol (9.40 mL)/ Et_3N (3.20 mL, 22.83 mmol). The desired product **7** was purified by silica gel column using a 6% ethyl acetate/hexane mixture. Brown oil, yield: 1.89 g (76%); $R_f=0.22$ (silica, CH_2Cl_2 /hexane 1:1); 1H NMR ($CDCl_3$, 500 MHz): $\delta=8.21$ (d, $J=8$ Hz, 1H), 7.91 (d, $J=7.5$ Hz, 2H), 7.87 (d, $J=8$ Hz, 1H), 7.77 (d, $J=7$ Hz, 1H), 7.50–7.60 (m, 3H), 7.38–7.44 (m, 4H), 5.16 (m, 1H), 4.85–4.93 (m, 2H), 3.60 ppm (m, 2H); ^{13}C NMR ($CDCl_3$, 125 MHz): $\delta=196.98, 136.39, 135.16, 134.24, 133.59, 133.09, 131.02, 129.28, 129.00, 128.75, 128.58, 128.48, 128.14, 128.07, 127.22, 126.97, 126.10, 125.62, 125.30, 123.53, 122.43, 78.86, 41.48, 33.65$ ppm; HRMS (ESI-Q-TOF): m/z calcd for $C_{20}H_{18}NO_3^+$: 320.1287 $[M]^+$; found: 320.1292.

Compound 8: Chalcone **2** (2 g, 7.56 mmol) and nitromethane (1.61 mL, 30.24 mmol) were reacted in a mixture of methanol (9.20 mL)/ Et_3N (3.10 mL, 22.3 mmol). The desired product **8** was purified by column chromatography on silica gel using a 6% ethyl acetate/hexane mixture. Yellow oil, yield: 1.34 g (54%); $R_f=0.20$ (silica, CH_2Cl_2 /hexane 1:1); 1H NMR ($CDCl_3$, 500 MHz): $\delta=8.20$ (d, $J=8.5$ Hz, 1H), 7.86 (d, $J=8$ Hz, 1H), 7.76 (m, 1H), 7.66 (d, $J=3.5$ Hz, 1H), 7.57–7.62 (m, 2H), 7.51 (m, 1H), 7.38–7.42 (m, 2H), 7.08 (d, $J=4.5$ Hz, 1H), 5.10–5.16 (m, 1H), 4.85–4.94 (m, 2H), 3.52 ppm (m, 2H); ^{13}C NMR ($CDCl_3$, 125 MHz): $\delta=189.83, 135.55, 134.86, 134.35, 124.23, 132.31, 130.99, 129.28, 128.54, 128.29, 127.00, 126.12, 125.31, 123.55, 122.40, 78.71, 42.02, 33.81$ ppm; HRMS (ESI-Q-TOF): m/z calcd for $C_{18}H_{16}NO_3S^+$: 326.0851 $[M]^+$; found: 326.0831.

Compound 9: Chalcone **3** (2.00 g, 5.35 mmol) and nitromethane (1.14 mL, 21.40 mmol) were reacted in a mixture of methanol (6.50 mL)/ Et_3N (2.20 mL, 15.78 mmol). The desired product **9** was purified by silica gel column chromatography using a 35% CH_2Cl_2 /hexane mixture. Pale yellow oil, yield: 1.47 g (63%); $R_f=0.19$ (silica, CH_2Cl_2 /hexane 1.5:1); 1H NMR ($CDCl_3$, 500 MHz): $\delta=8.12$ (d, $J=7.5$ Hz, 2H), 7.96 (d, $J=8$ Hz, 2H), 7.58–7.61 (m, 1H), 7.47–7.54 (m, 6H), 7.35–7.42 (m, 4H), 7.26–7.29 (m, 2H), 4.90–4.94 (m, 1H), 4.77–4.81 (m, 1H), 4.34–4.39 (m, 1H), 3.48–3.60 ppm (m, 2H); ^{13}C NMR ($CDCl_3$, 125 MHz): $\delta=196.68, 140.69, 138.30, 137.36, 136.34, 133.75, 129.05, 128.85, 128.10, 127.60, 125.98, 123.42, 120.33, 120.08, 109.75, 41.56, 39.01$ ppm; HRMS (ESI-Q-TOF): m/z calcd for $C_{28}H_{23}N_2O_3^+$: 435.1709 $[M+H]^+$; found: 435.1690.

Compound 10: Chalcone **4** (3.00 g, 7.90 mmol) and nitromethane (1.70 mL, 31.60 mmol) were reacted in a mixture of methanol (9.60 mL)/ Et_3N (3.20 mL, 23.30 mmol). The desired product **10** was purified by silica gel column using a 35% CH_2Cl_2 /hexane (35%) mixture. Pale yellow oil, yield: 2.13 g (61%); $R_f=0.18$ (silica, CH_2Cl_2 /hexane 1.5:1); 1H NMR ($CDCl_3$, 500 MHz): $\delta=8.12$ (d, $J=8$ Hz, 2H), 7.71 (d, $J=3$ Hz, 1H), 7.65 (m, 1H), 7.47–7.52 (m, 4H), 7.34–7.39 (m,

4H), 7.26 (m, 2H), 7.12 (m, 1H), 4.88–4.92 (m, 1H), 4.75–4.80 (m, 1H), 4.29–4.35 (m, 1H), 3.38–3.49 ppm (m, 2H); ^{13}C NMR ($CDCl_3$, 125 MHz): $\delta=189.7, 143.56, 140.73, 138.17, 138.15, 137.29, 134.60, 132.56, 129.12, 128.46, 127.52, 126.17, 123.49, 120.45, 120.27, 120.26, 109.92, 79.25, 42.13, 39.23$ ppm; HRMS (ESI-Q-TOF): m/z calcd for $C_{26}H_{21}N_2O_3S^+$: 441.1273 $[M+H]^+$; found: 441.1283.

Compound 11: Chalcone **5** (1.00 g, 2.82 mmol) and nitromethane (0.60 mL, 11.28 mmol) were reacted in a mixture of methanol (3.40 mL)/ Et_3N (1.16 mL, 8.3 mmol). The desired product **11** was purified by silica gel column using a 6% ethyl acetate/hexane mixture. Pale yellow oil, yield: 0.75 g (64%); $R_f=0.23$ (silica, CH_2Cl_2 /hexane 1:1); 1H NMR ($CDCl_3$, 500 MHz): $\delta=8.05$ (d, $J=8$ Hz, 1H), 7.97 (s, 1H), 7.91 (d, $J=7$ Hz, 2H), 7.53 (t, $J=7.5$ Hz, 1H), 7.40–7.46 (m, 3H), 7.31–7.37 (m, 3H), 7.19–7.23 (m, 1H), 4.89–4.92 (m, 1H), 4.74–4.88 (m, 1H), 4.40 (m, 1H), 4.23 (t, $J=7.5$ Hz, 2H), 3.47–3.60 (m, 2H), 1.80 (t, $J=7.5$ Hz, 2H), 1.32–1.38 (m, 2H), 0.92 ppm (t, $J=7.5$ Hz, 3H); ^{13}C NMR ($CDCl_3$, 125 MHz): $\delta=197.25, 140.89, 139.97, 136.62, 133.44, 128.71, 128.08, 125.97, 125.00, 123.24, 122.46, 120.44, 119.19, 118.96, 109.23, 108.87, 80.34, 42.92, 42.32, 31.15, 20.56, 13.88$ ppm; HRMS (ESI-Q-TOF): m/z calcd for $C_{26}H_{27}N_2O_3^+$: 415.2022 $[M]^+$; found: 415.2028.

Compound 12: Chalcone **6** (0.42 g, 1.17 mmol) and nitromethane (0.25 mL, 4.68 mmol) were dissolved in a mixture of methanol (1.50 mL)/ Et_3N (0.50 mL, 3.45 mmol). The desired product **12** was purified by silica gel column using a 6% ethyl acetate/hexane mixture. Pale yellow oil, yield: 0.25 g (51%); $R_f=0.22$ (silica, CH_2Cl_2 /hexane 1:1); 1H NMR ($CDCl_3$, 500 MHz): $\delta=8.70$ (d, $J=8$ Hz, 1H), 7.97 (s, 1H), 7.69 (d, $J=3.5$ Hz, 1H), 7.60 (d, $J=4.5$ Hz, 1H), 7.45 (t, $J=7.5$ Hz, 1H), 7.37 (d, $J=8.5$ Hz, 1H), 7.34 (s, 2H), 7.21 (t, $J=7.5$ Hz, 1H), 7.08 (m, 1H), 4.89–4.93 (m, 1H), 4.76–4.80 (m, 1H), 4.34–4.40 (m, 1H), 4.22–4.25 (m, 2H), 3.51 (m, 1H), 1.80 (q, $J=7.5$ Hz, 2H), 1.33–1.40 (m, 2H), 0.92 ppm (m, 3H); ^{13}C NMR ($CDCl_3$, 125 MHz): $\delta=190.21, 143.70, 140.83, 139.96, 134.26, 132.32, 129.01, 128.25, 125.95, 124.92, 123.17, 122.36, 120.41, 119.11, 118.92, 109.21, 108.83, 80.15, 50.69, 42.92, 39.83, 31.12, 20.54, 13.85$ ppm; HRMS (ESI-Q-TOF): m/z calcd for $C_{24}H_{25}N_2O_3S^+$: 421.1586 $[M+H]^+$; found: 421.1587.

General Procedure for Aza-dipyrins 13–18

The precursor compound (**7–12**; 1 equiv) was dissolved in ethanol (15 mL), and NH_4OAc (35 equiv) was added to it. The reaction mixture was allowed to stir for 48 h. Towards completion of the reaction, the product precipitated as blue solid. The crude product was filtered and washed with cold ethanol to obtain pure aza-dipyrin.

Compound 13: Compound **7** (2.26 g, 8.78 mmol) was treated with NH_4OAc (23.69 g, 307.43 mmol) in ethanol (20.00 mL) per the general procedure. Blue solid, yield: 1.42 g (29%); $R_f=0.24$ (silica, CH_2Cl_2 /hexane 1:1.5); 1H NMR ($CDCl_3$, 500 MHz): $\delta=8.28$ (d, $J=8$ Hz, 2H), 8.01 (d, $J=7.5$ Hz, 4H), 7.81 (d, $J=6.5$ Hz, 2H), 7.71 (d, $J=8$ Hz, 2H), 7.55–7.60 (m, 6H), 7.45–7.51 (m, 6H), 7.22 ppm (d, $J=6.5$ Hz, 4H); ^{13}C NMR ($CDCl_3$, 125 MHz): $\delta=154.99, 150.43, 142.49, 133.8, 132.27, 131.9, 131.18, 130.15, 129.67, 129.24, 128.3, 128.11, 126.65, 126.26, 125.86, 125.43, 125.03, 118.87$ ppm; HRMS (ESI-Q-TOF): m/z calcd for $C_{40}H_{28}N_3^+$: 550.2283 $[M+H]^+$; found: 550.2283.

Compound 14: Compound **8** (2.10 g, 1.69 mmol) and NH_4OAc (17.50 g, 227.17 mmol) were reacted in ethanol (20.00 mL) per the general procedure. Blue solid, yield: 0.43 g (11%); $R_f=0.22$ (silica, CH_2Cl_2 /hexane 1:1.5); 1H NMR ($CDCl_3$, 500 MHz): $\delta=8.24$ (d, $J=8.5$ Hz, 2H), 7.80 (d, $J=6.5$ Hz, 2H), 7.69 (d, $J=7$ Hz, 2H), 7.60 (d, $J=2.5$ Hz, 2H), 7.56 (d, $J=7$ Hz, 2H), 7.52 (d, $J=4.5$ Hz, 2H), 7.44 (m, 4H), 7.19–7.22 (m, 4H), 7.07 ppm (s, 2H); ^{13}C NMR ($CDCl_3$,

125 MHz): $\delta = 150.19, 149.02, 142.10, 137.19, 133.78, 131.86, 131.00, 129.62, 128.81, 128.78, 128.29, 128.14, 127.46, 126.23, 125.86, 25.43, 125.01, 118.72$ ppm; HRMS (ESI-Q-TOF): m/z calcd for $C_{36}H_{24}N_3S_2^+$: 562.1412 $[M+H]^+$; found: 562.1415.

Compound 15: Compound **9** (2.00 g, 4.6 mmol) and NH_4OAc (12.40 g, 161 mmol) were reacted in ethanol (20.00 mL) per the general procedure. Blue solid, yield: 1.04 g (29%); $R_f = 0.22$ (silica, CH_2Cl_2 /hexane 1:1); 1H NMR ($CDCl_3$, 500 MHz): $\delta = 8.33$ (d, $J = 7.5$ Hz, 4H), 8.09 (d, $J = 7.5$ Hz, 4H), 8.03 (d, $J = 7.5$ Hz, 4H), 7.65 (d, $J = 8$ Hz, 4H), 7.59 (t, $J = 7.5$ Hz, 4H), 7.53 (d, $J = 7$ Hz, 2H), 7.45 (d, $J = 8$ Hz, 4H), 7.32 (s, 2H), 7.19 (m, 4H), 7.14 ppm (m, 4H); ^{13}C NMR ($CDCl_3$, 125 MHz): $\delta = 155.50, 141.85, 140.65, 137.62, 132.70, 132.09, 130.54, 130.43, 130.37, 129.28, 126.69, 126.64, 123.53, 120.39, 120.24, 120.03, 115.51, 114.73, 109.96, 109.75$ ppm; HRMS (ESI-Q-TOF): m/z calcd for $C_{56}H_{38}N_5^+$: 780.3127 $[M+H]^+$; found: 780.3129.

Compound 16: Compound **10** (1.50 g, 3.28 mmol) and NH_4OAc (8.86 g, 114.98 mmol) were reacted in ethanol (20.00 mL) per the general procedure. Blue solid, yield: 0.47 g (18%); $R_f = 0.20$ (silica, CH_2Cl_2 /hexane 1:1); 1H NMR ($CDCl_3$, 500 MHz): $\delta = 8.30$ (d, $J = 8$ Hz, 4H), 8.08 (d, $J = 7.5$ Hz, 4H), 7.62–7.76 (m, 7H), 7.57 (d, $J = 5$ Hz, 2H), 7.43 (d, $J = 8$ Hz, 4H), 7.18 (m, 7H), 7.14 ppm (m, 4H); ^{13}C NMR ($CDCl_3$, 125 MHz): $\delta = 149.45, 141.45, 140.63, 137.62, 137.01, 132.53, 130.38, 129.10, 128.85, 127.62, 126.62, 125.99, 123.51, 120.23, 120.01, 115.06, 109.73$ ppm; HRMS (ESI-Q-TOF): m/z calcd for $C_{52}H_{34}N_5S_2^+$: 792.2256 $[M+H]^+$; found: 792.2230.

Compound 17: Compound **11** (0.70 g, 1.69 mmol) and NH_4OAc (4.55 g, 59.15 mmol) were reacted in ethanol (20.00 mL) per the general procedure. Blue solid, yield: 0.58 g (46%); $R_f = 0.22$ (silica, CH_2Cl_2 /hexane 1:2); 1H NMR ($CDCl_3$, 500 MHz): $\delta = 8.83$ (s, 2H), 8.34 (d, $J = 8.5$ Hz, 2H), 8.02 (d, $J = 8$ Hz, 4H), 7.88 (d, $J = 7.5$ Hz, 2H), 7.55 (t, $J = 7.5$ Hz, 4H), 7.46 (m, 2H), 7.35–7.41 (m, 4H), 7.31 (d, $J = 8.5$ Hz, 2H), 7.27 (s, 2H), 7.01 (t, $J = 7.5$ Hz, 2H), 4.20 (t, $J = 7.5$ Hz, 4H), 1.76–1.82 (m, 4H), 1.33–1.39 (m, 4H), 0.91 ppm (t, $J = 7.5$, 6H); ^{13}C NMR ($CDCl_3$, 125 MHz): $\delta = 154.83, 149.90, 143.89, 140.83, 140.41, 132.63, 129.72, 129.06, 127.17, 126.54, 125.49, 125.20, 123.30, 123.14, 120.72, 118.71, 113.41, 108.78, 108.63, 42.91, 31.13, 20.51, 13.84$ ppm; HRMS (ESI-Q-TOF): m/z calcd for $C_{52}H_{46}N_5^+$: 740.3753 $[M+H]^+$; found: 740.3720.

Compound 18: Compound **12** (1.00 g, 2.37 mmol) and NH_4OAc (6.40 g, 82.95 mmol) were reacted in ethanol (20.00 mL) per the general procedure. Blue solid, yield: 0.37 g (21%); $R_f = 0.21$ (silica, CH_2Cl_2 /hexane 1:2); 1H NMR ($CDCl_3$, 500 MHz): $\delta = 8.81$ (s, 2H), 8.32 (d, $J = 8.5$ Hz, 2H), 7.89 (d, $J = 7.5$ Hz, 2H), 7.65 (d, $J = 3.5$ Hz, 2H), 7.51 (d, $J = 5$ Hz, 2H), 7.35–7.41 (m, 4H), 7.31 (d, $J = 8.5$ Hz, 2H), 7.22 (t, $J = 4.5$ Hz, 2H), 7.13 (s, 2H), 7.02 (t, $J = 7.5$ Hz, 2H), 4.20 (t, $J = 7.5$ Hz, 4H), 1.76–1.82 (m, 4H), 1.32–1.38 (m, 4H), 0.90 ppm (t, $J = 7.5$ Hz, 6H); ^{13}C NMR ($CDCl_3$, 125 MHz): $\delta = 149.62, 148.89, 143.47, 140.81, 140.41, 137.60, 128.61, 128.22, 127.14, 126.90, 125.51, 125.02, 123.27, 123.11, 121.36, 120.77, 118.72, 113.32, 108.78, 108.66, 42.90, 31.14, 29.72, 20.51, 13.86$ ppm; HRMS (ESI-Q-TOF): m/z calcd for $C_{48}H_{42}N_5S_2^+$: 752.2882 $[M]^+$; found: 752.2860.

General Procedure for Aza-BODIPYs 19–24

In a clean, dry, two-necked, round-bottomed 100–250 mL flask, aza-dipyrrin (**19–24**, 1 equiv) was taken under inert atmosphere. Dry CH_2Cl_2 (11 equiv) and dry diisopropylethylamine (DIEA; 11 equiv) were added into the flask. After 15 min, $BF_3 \cdot OEt_2$ (15.6 equiv) was added to the reaction mixture and allowed to stir for 24 h at room temperature. The color of the reaction mixture changed from blue to green when the product formed, then it was quenched with water and extracted with dichloromethane. The solvent was dried over anhydrous Na_2SO_4 and evaporated using

a rotary evaporator before subjection to silica gel column chromatography.

Compound 19: Aza-dipyrrin **13** (0.2 g, 0.36 mmol) and $BF_3 \cdot OEt_2$ (0.71 mL, 5.61 mmol) were reacted in a mixture of dry CH_2Cl_2 (0.25 mL)/dry DIEA (0.7 mL) per the general procedure. The desired product was purified by column chromatography on silica gel and eluted with 40% CH_2Cl_2 /hexane. Evaporation of the solvent mixture afforded **19** as a metallic green solid. Yield: 0.05 g (23%); $R_f = 0.22$ (silica, CH_2Cl_2 /hexane 1:1.5); 1H NMR ($CDCl_3$, 500 MHz): $\delta = 8.27$ (d, $J = 9$ Hz, 2H), 8.13 (d, $J = 4.5$ Hz, 4H), 7.85 (m, 2H), 7.79 (d, $J = 8.5$ Hz, 2H), 7.66 (d, $J = 6.5$ Hz, 2H), 7.51 (m, 10H), 7.33 (t, $J = 8$ Hz, 2H), 7.12 ppm (s, 2H); ^{13}C NMR ($CDCl_3$, 125 MHz): $\delta = 159.35, 146.71, 144.40, 133.86, 131.65, 131.57, 131.01, 130.32, 129.81, 129.77, 129.45, 128.71, 128.54, 126.48, 125.83, 125.08, 123.14$ ppm; ^{19}F NMR (470.4 MHz, $CDCl_3$): $\delta = -131.59$ ppm (q, 2F); ^{11}B NMR (160 MHz, $CDCl_3$): $\delta = 1.18$ ppm (t, 1B); HRMS (ESI-Q-TOF): m/z calcd for $C_{40}H_{27}BF_2N_3^+$: 598.2266 $[M+H]^+$; found: 598.2244.

Compound 20: Aza-dipyrrin **14** (0.20 g, 0.35 mmol) and $BF_3 \cdot OEt_2$ (0.69 mL, 5.46 mmol) were reacted in a mixture of dry CH_2Cl_2 (0.25 mL)/dry DIEA (0.70 mL) per the general procedure. The desired product was purified by column chromatography on silica gel and eluted with 40% CH_2Cl_2 /hexane. Evaporation of the solvent mixture afforded **20** as a metallic green solid. Yield: 0.06 g (28%); $R_f = 0.19$ (silica, CH_2Cl_2 /hexane 1:1.5); 1H NMR ($CDCl_3$, 500 MHz): $\delta = 8.45$ (d, $J = 4$ Hz, 2H), 8.23 (d, $J = 7.5$ Hz, 2H), 7.84 (d, $J = 8.5$ Hz, 2H), 7.77 (d, $J = 8.5$ Hz, 2H), 7.67 (d, $J = 5$ Hz, 2H), 7.62 (d, $J = 7$ Hz, 2H), 7.48–7.53 (m, 4H), 7.28–7.31 (m, 2H), 7.25 ppm (d, $J = 5$ Hz, 4H); ^{13}C NMR ($CDCl_3$, 125 MHz): $\delta = 149.69, 146.71, 143.10, 134.16, 133.84, 133.33, 133.27, 133.21, 131.96, 131.65, 130.03, 129.90, 129.58, 129.35, 128.50, 126.44, 125.84, 125.79, 125.04, 122.63$ ppm; ^{19}F NMR (470.4 MHz, $CDCl_3$): $\delta = -139.32$ ppm (q, 2F); ^{11}B NMR (160 MHz, $CDCl_3$): $\delta = 1.47$ ppm (t, 1B); HRMS (ESI-Q-TOF): m/z calcd for $C_{36}H_{23}BF_2N_3S_2^+$: 610.1395 $[M+H]^+$; found: 610.1362.

Compound 21: Aza-dipyrrin **15** (0.50 g, 0.64 mmol) and $BF_3 \cdot OEt_2$ (1.26 mL, 9.98 mmol) were reacted in a mixture of dry CH_2Cl_2 (0.45 mL)/dry DIEA (1.30 mL) per the general procedure. The desired product **21** was purified by silica gel column chromatography using a 45% CH_2Cl_2 /hexane mixture. Green solid, yield: 0.08 g (15%); $R_f = 0.21$ (silica, CH_2Cl_2 /hexane 1:1); 1H NMR ($CDCl_3$, 500 MHz): $\delta = 8.91$ (s, 2H), 8.35 (dd, $J = 8.5$ Hz, $J = 1.5$ Hz, 2H), 8.09 (m, 4H), 7.99 (d, $J = 8.5$ Hz, 2H), 7.47–7.51 (m, 6H), 7.39–7.44 (m, 6H), 7.07 (m, 4H), 4.26 (d, $J = 7.5$ Hz, 4H), 1.80–1.86 (m, 4H), 1.34–1.42 (m, 4H), 0.93 ppm (t, $J = 7.5$, 6H); ^{13}C NMR ($CDCl_3$, 125 MHz): $\delta = 151.75, 140.60, 130.42, 129.29, 126.68, 126.63, 126.00, 120.25, 120.02, 115.20, 109.74, 52.34$ ppm; ^{19}F NMR (470.4 MHz, $CDCl_3$): $\delta = -131.18$ ppm (q, 2F); ^{11}B NMR (160 MHz, $CDCl_3$): $\delta = 1.04$ ppm (t, 1B); HRMS (ESI-Q-TOF): m/z calcd for $C_{56}H_{37}BF_2N_5^+$: 828.3110 $[M+H]^+$; found: 828.3121.

Compound 22: Aza-dipyrrin **16** (0.32 g, 0.4 mmol) and $BF_3 \cdot OEt_2$ (0.79 mL, 6.24 mmol) were reacted in a mixture of dry CH_2Cl_2 (0.30 mL)/dry DIEA (0.80 mL) per the general procedure. The desired product **22** was purified by silica gel column chromatography using a 45% CH_2Cl_2 /hexane mixture. Green solid, yield: 0.05 g (14%); $R_f = 0.19$ (silica, CH_2Cl_2 /hexane 1:1); 1H NMR ($CDCl_3$, 500 MHz): $\delta = 8.44$ (d, $J = 4$ Hz, 2H), 8.31 (d, $J = 8$ Hz, 4H), 8.09 (m, 4H), 7.68 (m, 6H), 7.47 (m, 4H), 7.31 (m, 2H), 7.28 (s, 2H), 7.23 ppm (m, 8H); ^{13}C NMR ($CDCl_3$, 125 MHz): $\delta = 150.06, 145.80, 141.81, 140.42, 138.92, 134.08, 133.42, 133.36, 132.08, 130.91, 130.69, 130.01, 126.70, 126.11, 123.69, 120.35, 120.28, 118.66, 109.75$ ppm; ^{19}F NMR (470.4 MHz, $CDCl_3$): $\delta = -138.58$ ppm (q, 2F); ^{11}B NMR (160 MHz, $CDCl_3$): $\delta = 1.37$ ppm (t, 1B); HRMS (ESI-Q-TOF): m/z calcd for $C_{52}H_{33}BF_2N_5S_2^+$: 840.2238 $[M+H]^+$; found: 840.2207.

Compound 23: Aza-dipyrrin **17** (0.50 g, 0.67 mmol) and $\text{BF}_3\cdot\text{OEt}_2$ (1.32 mL, 10.45 mmol) were reacted in a mixture of dry CH_2Cl_2 (0.50 mL)/dry DIEA (1.30 mL) per the general procedure. The desired product **23** was purified by silica gel column chromatography using a 30% CH_2Cl_2 /hexane mixture. Green solid, yield: 0.13 g (23%); $R_f=0.19$ (silica, CH_2Cl_2 /hexane 1:2); $^1\text{H NMR}$ (CDCl_3 , 500 MHz): $\delta=8.91$ (s, 2H), 8.34 (m, 2H), 8.09 (m, 4H), 7.99 (d, $J=7.5$ Hz, 2H), 7.47–7.51 (m, 6H), 7.39–7.44 (m, 6H), 7.07 (m, 4H), 4.26 (t, $J=7.5$ Hz, 4H), 1.80–1.86 (m, 4H), 1.34–1.42 (m, 4H), 0.93 ppm (t, $J=7.5$, 6H); $^{13}\text{C NMR}$ (CDCl_3 , 125 MHz): $\delta=158.59$, 151.75, 145.51, 145.07, 141.30, 140.95, 132.22, 130.42, 129.52, 128.49, 127.40, 126.03, 124.00, 123.55, 123.23, 122.16, 120.83, 119.26, 117.19, 109.21, 108.99, 43.04, 31.17, 20.53, 13.86 ppm; $^{19}\text{F NMR}$ (470.4 MHz, CDCl_3): $\delta=-130.38$ ppm (q, 2F); $^{11}\text{B NMR}$ (160 MHz, CDCl_3): $\delta=1.05$ ppm (t, 1B); HRMS (ESI-Q-TOF): m/z calcd for $\text{C}_{52}\text{H}_{45}\text{BF}_2\text{N}_5^+$: 788.3736 $[M+H]^+$; found: 788.3718.

Compound 24: Aza-dipyrrin **18** (0.20 g, 0.26 mmol) and $\text{BF}_3\cdot\text{OEt}_2$ (0.51 mL, 4.05 mmol) were reacted in a mixture of dry CH_2Cl_2 (0.20 mL)/dry DIEA (0.50 mL) per the general procedure. The desired product **24** was purified by silica gel column chromatography using a 30% CH_2Cl_2 /hexane mixture. Green solid, yield: 0.06 g (28%); $R_f=0.18$ (silica, CH_2Cl_2 /hexane 1:2); $^1\text{H NMR}$ (CDCl_3 , 500 MHz): $\delta=8.90$ (s, 2H), 8.41 (d, $J=3.5$ Hz, 2H), 8.35 (m, 2H), 8.00 (d, $J=8$ Hz, 2H), 7.61 (d, $J=5$ Hz, 2H), 7.39–7.44 (m, 6H), 7.28 (m, 2H), 7.23 (s, 2H), 7.05 (m, 2H), 4.27 (m, 4H), 1.81–1.87 (m, 4H), 1.34–1.42 (m, 4H), 0.92 ppm (m, 6H); $^{13}\text{C NMR}$ (CDCl_3 , 125 MHz): $\delta=149.05$, 145.76, 143.64, 141.20, 140.91, 134.58, 132.53, 132.46, 132.40, 130.65, 129.61, 127.27, 125.94, 123.71, 123.45, 123.23, 121.94, 120.88, 119.18, 116.69, 109.09, 108.92, 42.97, 31.14, 20.50, 13.83 ppm; $^{19}\text{F NMR}$ (470.4 MHz, CDCl_3): $\delta=-137.34$ ppm (q, 2F); $^{11}\text{B NMR}$ (160 MHz, CDCl_3): $\delta=1.30$ ppm (t, 1B); HRMS (ESI-Q-TOF): m/z calcd for $\text{C}_{48}\text{H}_{41}\text{BF}_2\text{N}_5\text{S}_2^+$: 800.2864 $[M]^+$; found: 800.2874.

CCDC-1016009 (**13**) and 1425995 (**14**) contain the supplementary crystallographic data for this paper. These data can be obtained free of charge from The Cambridge Crystallographic Data Centre via www.ccdc.cam.ac.uk/data_request/cif.

Acknowledgements

Financial support from the Science and Engineering Research Board (SERB) (EMR/2015/000779) of the Government of India, is greatly acknowledged. I.G. thanks Prof. H. Furuta of Kyushu University, Japan for X-ray measurements. N.B. thanks IIT Gandhinagar for a fellowship and infrastructural support. P. C. J. acknowledges CUG for providing basic computational facilities and UGC, New Delhi for startup grants. M.Y.L. thanks the UGC for financial assistance.

Keywords: density functional calculations • donor–acceptor systems • dyes/pigments • energy transfer • X-ray diffraction

- [1] a) N. S. Lewis, D. G. Nocera, *Proc. Natl. Acad. Sci. USA* **2006**, *103*, 15729–15735; b) G. D. Scholes, G. R. Fleming, A. Olaya-Castro, R. van Grondelle, *Nat. Chem.* **2011**, *3*, 763–774.
[2] a) I. Gupta, M. Ravikanth, *J. Org. Chem.* **2004**, *69*, 6796–6811; b) J. Wojaczyński, L. Latos-Grażyński, *Coord. Chem. Rev.* **2000**, *204*, 113–171; c) S. I. Yang, J. Seth, T. Balasubramanian, D. Kim, J. S. Lindsey, D. Holten, D. F. Bocian, *J. Am. Chem. Soc.* **1999**, *121*, 4008–4018; d) J. S. Hsiao, B. P. Krueger, R. W. Wagner, T. E. Johnson, J. K. Delaney, D. C. Mauzerall, G. R. Fleming, J. S. Lindsey, D. F. Bocian, R. J. Donohoe, *J. Am. Chem. Soc.* **1996**, *118*, 11181–11193; e) A. Osuka, N. Tanabe, S. Kawabata, I. Yamazaki, Y. Nishimura, *J. Org. Chem.* **1995**, *60*, 7177–7185.

- [3] a) G. Bottari, G. de La Torre, D. M. Guldi, T. Torres, *Chem. Rev.* **2010**, *110*, 6768–6816; b) A. Satake, Y. Kobuke, *Org. Biomol. Chem.* **2007**, *5*, 1679–1691.
[4] a) T. K. Khan, M. Bröring, S. Mathur, M. Ravikanth, *Coord. Chem. Rev.* **2013**, *257*, 2348–2387; b) F. Li, S. I. Yang, Y. Ciringh, J. Seth, C. H. Martin, D. L. Singh, D. Kim, R. R. Birge, D. F. Bocian, D. Holten, J. S. Lindsey, *J. Am. Chem. Soc.* **1998**, *120*, 10001–10017; c) D. Holten, D. F. Bocian, J. S. Lindsey, *Acc. Chem. Res.* **2002**, *35*, 57–69; d) T. K. Khan, M. Ravikanth, *Tetrahedron* **2011**, *67*, 5816–5824; e) T. K. Khan, M. Ravikanth, *Tetrahedron* **2012**, *68*, 830–840; f) M. Benstead, G. H. Mehl, R. W. Boyle, *Tetrahedron* **2011**, *67*, 3573–3601.
[5] a) A. Loudet, K. Burgess, *Chem. Rev.* **2007**, *107*, 4891–4932; b) A. Kamkaew, S. H. Lim, H. B. Lee, L. V. Kiew, L. Y. Chung, K. Burgess, *Chem. Soc. Rev.* **2013**, *42*, 77–88.
[6] a) V. Lakshmi, M. Ravikanth, *Dyes Pigm.* **2013**, *96*, 665–671; b) T. K. Khan, S. K. Jana, M. R. Rao, M. S. Shaikh, M. Ravikanth, *Inorg. Chim. Acta* **2012**, *383*, 257–266.
[7] a) H. Kim, A. Burghart, M. B. Welch, J. Reibenspies, K. Burgess, *Chem. Commun.* **1999**, 1889–1890; b) Y. Tomimori, T. Okujima, T. Yano, S. Mori, N. Ono, H. Yamada, H. Uno, *Tetrahedron* **2011**, *67*, 3187–3193; c) C. Ikeda, S. Ueda, T. Nabeshima, *Chem. Commun.* **2009**, 2544–2546; d) C. Ikeda, T. Maruyama, T. Nabeshima, *Tetrahedron Lett.* **2009**, *50*, 3349–3351.
[8] a) L. H. Thoresen, H. Kim, M. B. Welch, A. Burghart, K. Burgess, *Synlett* **1998**, *11*, 1276–1278; b) A. Burghart, H. Kim, M. B. Welch, L. H. Thoresen, J. Reibenspies, K. Burgess, F. Bergström, L. B. Å. Johansson, *J. Org. Chem.* **1999**, *64*, 7813–7819; c) K. Rurack, M. Kollmannsberger, J. Daub, *New J. Chem.* **2001**, *25*, 289–292; d) L. Huang, X. Yu, W. Wu, J. Zhao, *Org. Lett.* **2012**, *14*, 2594–2597; e) C. W. Wan, A. Burghart, J. Chen, F. Bergstrom, L. B. Johansson, M. F. Wolford, T. G. Kim, M. R. Topp, R. M. Hochstrasser, K. Burgess, *Chem. Eur. J.* **2003**, *9*, 4430–4441; f) O. Buyukcakil, O. A. Bozdemir, S. Kolemen, S. Erbas, E. U. Akkaya, *Org. Lett.* **2009**, *11*, 4644–4647.
[9] a) P. E. Kesavan, I. Gupta, *Dalton Trans.* **2014**, *43*, 12405–12413; b) P. E. Kesavan, S. Das, M. Y. Lone, P. C. Jha, S. Mori, I. Gupta, *Dalton Trans.* **2015**, *44*, 17209–17221.
[10] a) M. Tasiar, D. F. O’Shea, *Bioconjugate Chem.* **2010**, *21*, 1130–1133; b) M. Grossi, A. Palma, S. O. McDonnell, M. J. Hall, D. K. Rai, J. Muldoon, D. F. O’Shea, *J. Org. Chem.* **2012**, *77*, 9304–9312; c) H. Lu, S. Shimizu, J. Mack, Z. Shen, N. Kobayashi, *Chem. Asian J.* **2011**, *6*, 1026–1037.
[11] a) Q. Bellier, F. Dalier, E. Jeanneau, O. Maury, C. Andraud, *New J. Chem.* **2012**, *36*, 768–773; b) X. Zhang, H. Yu, Y. Xiao, *J. Org. Chem.* **2012**, *77*, 669–673; c) R. Gresser, H. Hartmann, M. Wrackmeyer, K. Leo, M. Riede, *Tetrahedron* **2011**, *67*, 7148–7155; d) J. Liu, Z. Yang, X. Liu, Z. Wang, Y. Liu, S. Bai, L. Lin, X. Feng, *Org. Biomol. Chem.* **2009**, *7*, 4120.
[12] a) S. O. McDonnell, D. F. O’Shea, *Org. Lett.* **2006**, *8*, 3493–3496; b) A. Coskun, M. D. Yilmaz, E. U. Akkaya, *Org. Lett.* **2007**, *9*, 607–609; c) R. E. Gawley, H. Mao, M. M. Haque, J. B. Thorne, J. S. Pharr, *J. Org. Chem.* **2007**, *72*, 2187–2191; d) S. Liu, Z. Shi, W. Xu, H. Yang, N. Xi, X. Liu, Q. Zhao, W. Huang, *Dyes Pigm.* **2014**, *103*, 145–153; e) J. Tian, J. Zhou, Z. Shen, L. Ding, J.-S. Yu, H. Ju, *Chem. Sci.* **2015**, *6*, 5969–5977.
[13] a) V. Bandi, M. E. El-Khouly, K. Ohkubo, V. N. Nesterov, M. E. Zandler, S. Fukuzumi, F. D’Souza, *J. Phys. Chem. C* **2014**, *118*, 2321–2332; b) V. Bandi, M. E. El-Khouly, V. N. Nesterov, P. A. Karr, S. Fukuzumi, F. D’Souza, *J. Phys. Chem. C* **2013**, *117*, 5638–5649.
[14] A. Loudet, R. Bandichhor, L. Wu, K. Burgess, *Tetrahedron* **2008**, *64*, 3642–3654.
[15] a) X. Peng, Z. Yang, J. Wang, J. Fan, Y. He, F. Song, B. Wang, S. Sun, J. Qu, J. Qi, M. Yan, *J. Am. Chem. Soc.* **2011**, *133*, 6626–6635; b) T. Myochin, K. Kiyose, K. Hanaoka, H. Kojima, T. Terai, T. Nagano, *J. Am. Chem. Soc.* **2011**, *133*, 3401–3409.
[16] a) J. Murtagh, D. O. Frimannsson, D. F. O’Shea, *Org. Lett.* **2009**, *11*, 5386–5389; b) A. Palma, M. Tasiar, D. O. Frimannsson, T. T. Vu, R. Méallet-Reault, D. F. O’Shea, *Org. Lett.* **2009**, *11*, 3638–3641; c) D. Collado, Y. Vida, F. Najera, E. Perez-Inestrosa, *RSC Adv.* **2014**, *4*, 2306–2309; d) W. Zheng, B.-B. Wang, C.-H. Li, J.-X. Zhang, C.-Z. Wan, J.-H. Huang, J. Liu, Z. Shen, X.-Z. You, *Angew. Chem. Int. Ed.* **2015**, *54*, 9070–9074; *Angew. Chem.* **2015**, *127*, 9198–9202; e) H. Lu, J. Mack, Y. Yanga, Z. Shen, *Chem. Soc. Rev.* **2014**, *43*, 4778–4823.
[17] T. Mueller, R. Gresser, K. Leo, M. Riede, *Sol. Energ. Mater. Sol.* **2012**, *99*, 176–181.

- [18] a) K. Flavin, K. Lawrence, J. Bartelmess, M. Tasiar, C. Navio, C. Bittencourt, D. F. O'Shea, D. M. Guldi, S. Giordani, *ACS Nano* **2011**, *5*, 1198–1206; b) A. Gorman, J. Killoran, C. O'Shea, T. Kenna, W. M. Gallagher, D. F. O'Shea, *J. Am. Chem. Soc.* **2004**, *126*, 10619–10631; c) D. O. Frimannsson, M. Grossi, J. Murtagh, F. Paradisi, D. F. O'Shea, *J. Med. Chem.* **2010**, *53*, 7337–7343.
- [19] a) Q. Bellier, S. Pégaz, C. Aronica, B. L. Guennic, C. Andraud, O. Maury, *Org. Lett.* **2011**, *13*, 22–25; b) A. Loudet, R. Bandichhor, K. Burgess, A. Palma, S. O. McDonnell, M. J. Hall, D. F. O'Shea, *Org. Lett.* **2008**, *10*, 4771–4774; c) J. Killoran, L. Allen, J. F. Gallagher, W. M. Gallagher, D. F. O'Shea, *Chem. Commun.* **2002**, 1862–1863; d) L. Jiao, Y. Wu, S. Wang, X. Hu, P. Zhang, C. Yu, K. Cong, Q. Meng, E. Hao, M. G. H. Vicente, *J. Org. Chem.* **2014**, *79*, 1830–1835; e) X. D. Jiang, Y. Fu, T. Zhang, W. Zhao, *Tetrahedron Lett.* **2012**, *53*, 5703–5706.
- [20] a) J. M. Chong, L. Shen, N. J. Taylor, *J. Am. Chem. Soc.* **2000**, *122*, 1822–1823; b) R. V. Syutkin, G. G. Abashev, E. V. Shklyayeva, P. G. Kudryavtsev, *Russ. J. Org. Chem.* **2011**, *47*, 530–536; c) K. Maria, H. L. Dimitra, G. Maria, *Med. Chem.* **2008**, *4*, 586–596; d) J. Z. Liu, S. E. Zhang, F. Nie, Y. Yang, Y. B. Tang, W. Yin, J. Y. Tian, F. Ye, Z. Xiao, *Bioorg. Med. Chem. Lett.* **2013**, *23*, 6217–6222.
- [21] C. J. Ziegler, K. Chanawanno, A. Hasheminsasab, Y. V. Zatsikha, E. Maligaspe, V. N. Nemykin, *Inorg. Chem.* **2014**, *53*, 4751–4755.
- [22] W. Qin, M. Baruah, M. Van der Auweraer, F. C. De Schryver, N. Boens, *J. Phys. Chem. A* **2005**, *109*, 7371–7384.
- [23] a) A. Costela, I. García-Moreno, C. Gomez, R. Sastre, F. Amat-Guerri, M. Liras, F. L. Arbeloa, J. B. Prieto, I. L. Arbeloa, *J. Phys. Chem. A* **2002**, *106*, 7736–7742; b) M. Kollmannsberger, K. Rurack, U. Resch-Genger, J. Daub, *J. Phys. Chem. A* **1998**, *102*, 10211–10220; c) J. B. Prieto, F. L. Arbeloa, V. M. Martinez, T. A. López, F. Amat-Guerri, M. Liras, I. L. Arbeloa, *Chem. Phys. Lett.* **2004**, *385*, 29–35.
- [24] a) C. Thivierge, J. Han, R. M. Jenkins, K. Burgess, *J. Org. Chem.* **2011**, *76*, 5219–5228; b) N. Balsukuri, S. Das, I. Gupta, *New J. Chem.* **2015**, *39*, 482–491.
- [25] Gaussian 09, Revision A.02, M. J. Frisch, G. W. Trucks, H. B. Schlegel, G. E. Scuseria, M. A. Robb, J. R. Cheeseman, G. Scalmani, V. Barone, B. Men-
nucci, G. A. Petersson, H. Nakatsuji, M. Caricato, X. Li, H. P. Hratchian, A. F. Izmaylov, J. Bloino, G. Zheng, J. L. Sonnenberg, M. Hada, M. Ehara, K. Toyota, R. Fukuda, J. Hasegawa, M. Ishida, T. Nakajima, Y. Honda, O. Kitao, H. Nakai, T. Vreven, J. A. Montgomery, Jr., J. E. Peralta, F. Ogliaro, M. Bearpark, J. J. Heyd, E. Brothers, K. N. Kudin, V. N. Staroverov, R. Kobayashi, J. Normand, K. Raghavachari, A. Rendell, J. C. Burant, S. S. Iyengar, J. Tomasi, M. Cossi, N. Rega, J. M. Millam, M. Klene, J. E. Knox, J. B. Cross, V. Bakken, C. Adamo, J. Jaramillo, R. Gomperts, R. E. Stratmann, O. Yazyev, A. J. Austin, R. Cammi, C. Pomelli, J. W. Ochterski, R. L. Martin, K. Morokuma, V. G. Zakrzewski, G. A. Voth, P. Salvador, J. J. Dannenberg, S. Dapprich, A. D. Daniels, O. Farkas, J. B. Foresman, J. V. Ortiz, J. Cio-slawski, D. J. Fox, Gaussian Inc., Wallingford CT, **2009**.
- [26] a) C. Adamo, V. Barone, *J. Chem. Phys.* **1999**, *110*, 6158–6170; b) M. Ernzerhof, G. E. Scuseria, *J. Chem. Phys.* **1999**, *110*, 5029–5036.
- [27] a) E. Runge, E. K. U. Gross, *Phys. Rev. Lett.* **1984**, *52*, 997–1000; b) M. E. Casida, in *Time-Dependent Density-Functional Response Theory for Molecules* (Ed.: D. P. Chong), World Scientific, Singapore, **1995**, *1*, 155–192.
- [28] A. D. Boese, J. M. L. Martin, *J. Chem. Phys.* **2004**, *121*, 3405–3416.
- [29] a) V. Barone, M. Cossi, *J. Phys. Chem. A* **1998**, *102*, 1995–2001; b) M. Cossi, N. Rega, G. Scalmani, V. Barone, *J. Comput. Chem.* **2003**, *24*, 669–681.
- [30] B. Le Guennic, O. Maury, D. Jacquemin, *Phys. Chem. Chem. Phys.* **2012**, *14*, 157–164.
- [31] M. R. Rao, K. V. P. Kumar, M. Ravikanth, *J. Organomet. Chem.* **2010**, *695*, 863–869.
- [32] W. Hong, B. Sun, H. Aziz, W. T. Park, Y. Y. Noh, Y. Li, *Chem. Commun.* **2012**, *48*, 8413–8415.
- [33] L. Leonat, G. Sbarcea, I. V. Branzoi, *U. P. B. Sci. Bull. Ser. B* **2013**, *75*, 111–118.

Manuscript received: February 10, 2016

Accepted Article published: February 25, 2016

Final Article published: April 8, 2016